Syst. Biol. 75(3):468–492, 2026

https://doi.org/10.1093/sysbio/syaf064
Advance Access publication September 25, 2025

Integrating Genomics, Collections, and Community Science to Delimit Species Clarifies the Taxonomy of a Variable Monitor Lizard (*Varanus tristis)*

Carlos J. Pavón-Vázquez [1,2,*], Alison J. Fitch[3], Paul Doughty[4], Stephen C. Donnellan [5], and J. Scott Keogh[2]

[1]*Facultad de Estudios Superiores Iztacala, Universidad Nacional Autónoma de México, Avenida de los Barrios 1, Colonia Los Reyes Ixtacala, Tlalnepantla, Estado de México, C.P. 54090, Mexico*

[2]*Division of Ecology and Evolution, Research School of Biology, The Australian National University, 46 Sullivans Creek Road, Canberra, ACT 2600, Australia*

[3]*College of Science and Engineering, Flinders University, Physical Sciences Building, Anchor Court, Bedford Park, SA 5042, Australia*

[4]*Collections & Research, Western Australian Museum, 49 Kew St, Welshpool, WA 6160, Australia*

[5]*Research and Collections, South Australian Museum, North Terrace, Adelaide, SA 5000, Australia*

[*]*Correspondence to be sent to: Facultad de Estudios Superiores Iztacala, Universidad Nacional Autónoma de México, Colonia Los Reyes Ixtacala, Tlalnepantla, Estado de México, C.P. 54090, Mexico; E-mail: cjpvunam@gmail.com*

Received 4 October 2023; reviews returned 2 September 2025; accepted 10 September 2025
Associate Editor: Rayna Bell

Abstract.—The accurate characterization of species diversity is a vital prerequisite for ecological and evolutionary research, as well as conservation. Thus, it is necessary to generate robust hypotheses of species limits based on the inference of evolutionary processes. Integrative species delimitation, the inference of species limits based on multiple sources of evidence, can provide unique insight into species diversity and the processes behind it. Here, we show how community observations can be integrated with standard molecular and phenotypic data sets under an integrative framework to identify the processes generating genetic and phenotypic variation. We implement this approach in *Varanus tristis*, a widespread and variable complex of Australian monitor lizards. Using genomic, phenotypic (linear and geometric morphometrics, coloration), spatial, and environmental data, we show that disparity in this complex is inconsistent with intraspecific variation and instead suggests that speciation has occurred. Based on our results, we provide an updated taxonomy for this complex and identify the processes that may have been responsible for the geographic sorting of variation. Our workflow provides a guideline for the integrative analysis of several types of data to identify the occurrence and causes of speciation. Furthermore, our study highlights the benefits and caveats associated with community science and machine learning—two tools used here—in taxonomic research. [Australia; coloration; citizen science; machine learning; morphometrics; integrative taxonomy; phylogenomics; species delimitation.]

The mischaracterization of species diversity poses a major challenge to our understanding of the ecology, evolution, and conservation of biodiversity (Bini et al. 2006; Hortal et al. 2015). Therefore, generating accurate species delimitation hypotheses is a crucial goal of systematic biology. The rapid accumulation of large molecular data sets for nonmodel organisms has proven to be a valuable tool in this quest. First, high-throughput sequencing may allow the detection of cryptic species in cases where morphology or smaller molecular data sets fail to provide evidence for speciation (Weiss et al. 2018). Second, a wider genome representation may reveal complex gene flow scenarios that would remain undetected by other types of data alone, thereby preventing the overestimation of species diversity (Hinojosa et al. 2019; Chan et al. 2020).

Although large molecular data sets provide a plethora of information, there are caveats that need to be taken into consideration when using them for species delimitation. With increasing data there is the potential to detect finer-scale population structure, which can be misidentified as species-level divergence by some species delimitation approaches (Sukumaran and Knowles 2017). Isolation by distance (IBD)—the positive correlation between genetic and geographic distance—is common in natural populations and can confound species delimitation (Mason et al. 2020). Isolation by environment (IBE) may also misguide species delimitation and could be even more common than IBD (Sexton et al. 2014). Gene flow and incomplete lineage sorting are other common sources of uncertainty and conflict in species delimitation (Weber et al. 2019; Chan et al. 2020).

One way to minimize the impact of the shortcomings of the different methods and data is to implement integrative species delimitation, analyzing multiple sources of evidence in different ways. The implementation of integrative taxonomy often minimizes over-splitting if species status is reliant on the congruence between data and approaches (Carstens et al. 2013). In this context, morphological data remain a valuable source of information. The phenotype embodies a plethora of

biological information, reflecting characteristics of the genotype, gene interactions, epigenetic regulation, and environmental demands. The approaches used to collect and analyze morphological data have advanced in parallel to molecular methods, providing unique insight into species limits (Pavón-Vázquez et al. 2018, 2022; Chaplin et al. 2020). Furthermore, museum specimens link specific phenotypes (and genotypes, if molecular resources are available) with specific temporal, geographic, and environmental conditions (Edwards et al. 2005; Schmitt et al. 2019). In that way, they can provide valuable insight into the drivers of genotypic and phenotypic divergence. Thus, the development of approaches that can integrate multiple sources of evidence to inform taxonomy (e.g., Solís-Lemus et al. 2015; Pyron 2023) is crucial.

Compared with molecular and morphological data from museum specimens, observations made by the general public remain a largely underutilized resource in taxonomic research. Biodiversity community science projects and observations are accumulating rapidly (Pocock et al. 2017; Rowley et al. 2019; Messaglio and Callahan 2021), generating valuable data for understudied taxa and regions. Community observations—with iNaturalist (https://www.inaturalist.org/) as their best-known repository—have been mainly leveraged in the context of conservation (McKinley et al. 2017; Chowdhury et al. 2023b). However, these observations also convey important information about the geographic and temporal distribution of morphological variation (Drury et al. 2019; Hantak et al. 2022). In this way, community science can inform taxonomy by uncovering undescribed species (Zhang et al. 2022; Manley et al. 2025) and providing important insights into evolutionary processes (Fritz and Ihlow 2022; Fritz et al. 2023; Pizarro et al. 2023).

Morphologically variable species complexes represent a challenge for traditional species delimitation approaches. Geographic patterns of morphological variation may lead to overestimation of species diversity (Padula et al. 2016) or prove too complex to be easily translatable into binomial nomenclature (Mallet 2007). Molecular data can also result in inaccurate delimitations, especially if patterns of gene flow/isolation are not adequately characterized (Pyron et al. 2022; Pavón-Vázquez et al. 2024; Chambers et al. 2025). One such variable species complex with a controversial taxonomy is the monitor lizard *Varanus tristis* (Fig. 1a). This lizard has one of the widest distributions among Australian reptiles: its range encompasses most of the continent, except for the coldest regions in the south (Figs. 1b, c) (Pianka 1971, 2004). The species exhibits considerable variation throughout its range. Dark-headed individuals are found in the central and western portions of the range. The bodies of these individuals show varying degrees of melanism, with darker colors becoming more prevalent in southern Australia (Pianka 2004; Schmida 2020). Light-headed individuals are known from the northern Monsoonal Tropics and adjacent areas in eastern Australia (Pianka 2004; Schmida 2020). This phenotype is also predominant in Asutralia's Central Ranges, with a few isolated records from other parts of the country dominated by dark-headed individuals (pers. obs.). Light-headed individuals show variation in the extent

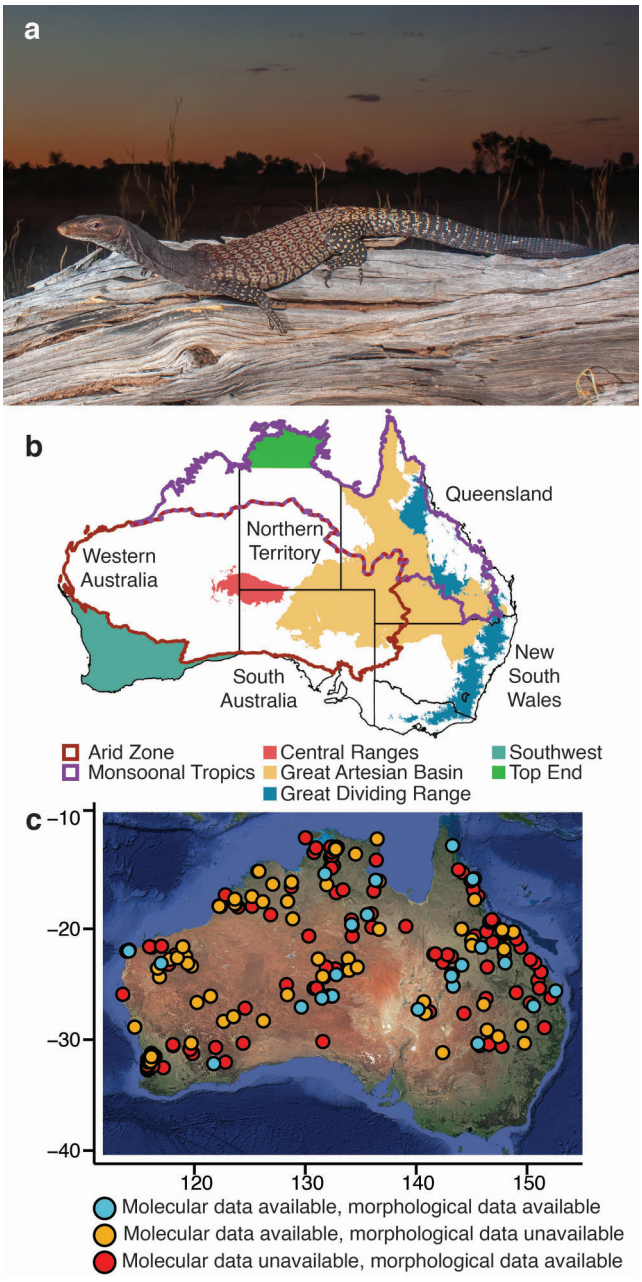

FIGURE 1. Focal taxon and study area. a) Adult male *V. tristis* from central Queensland, Australia; photograph by Kieran Palmer. b) Mainland Australia; black lines indicate state borders, with names next to them; other regions mentioned throughout the text are indicated by the colored polygons. c) Sampling of *V. tristis*; colored circles indicate the major types of data available for each individual; base map ©2023 Google.

and conspicuousness of eye-like markings (ocelli), as well as in head color (ranging from brownish-gray to yellowish/reddish). Additionally, individuals occurring east of the Great Dividing Range show a unique combination of coloration, scale characters (scutellation), and morphometric traits (Storr 1980; Pianka 2004; Schmida 2020).

The phenotypic variation detailed above has led to the recognition of 2 subspecies within *V. tristis*: *V. tristis tristis* and *V. tristis orientalis*. However, authors disagree on which populations should be assigned to each subspecies. Some authors apply the name *V. t. tristis* to all dark-headed individuals and *V. t. orientalis* to the light-headed individuals from the Monsoonal Tropics and eastern Australia (Pianka 2004; Cogger 2014), apparently unaware of the presence of light-headed lizards in the Central Ranges and occasionally elsewhere. Other authors reserve the use of *V. t. orientalis* for the morphologically unique, light-headed individuals occurring east of the Great Dividing Range (e.g., Storr 1980; Schmida 2020). By contrast, most Australian zoological collections (Online Zoological Collections of Australian Museums 2025) and the Australian Society of Herpetologists Official List of Australian Species (2025) do not recognize subspecies within *V. tristis* because of a lack of reciprocal monophyly between light- and dark-headed individuals in a mitochondrial study (Fitch et al. 2006) and the morphological intergradation between them (Pianka 2004). Ultimately, taxonomic clarity in these monitors is hindered by the lack of any comprehensive analysis of genetic and morphological variation.

Here, we present an integrative workflow to delimit species that capitalizes on the wealth of samples and information available in public repositories (Fig. 1c). In particular, it uses a combination of molecular, environmental, and phenotypic data obtained from tissue samples, museum specimens, and innovatively from community observations. The data are analyzed both iteratively (i.e., in separate steps) and integratively (i.e., simultaneously) to identify evolutionarily independent lineages using several tools, including machine learning. We demonstrate the utility of this workflow for species delimitation in taxonomically contentious complexes by applying it to *V. tristis*. Our analyses support differentiation due to speciation rather than intraspecific variation and provide the basis for an updated taxonomy for these variable monitor lizards.

Materials and Methods

Our workflow has characteristics of both iterative and integrative species delimitation (Fig. 2). First, we identified clusters of individuals using a variety of approaches and data to generate primary hypotheses of species limits, which were then tested for specific status using downstream analyses. Second, we used common approaches for molecular species delimitation to evaluate the genetic divergence between the clusters, supported by phylogenetic methods. Third, we characterized the geographic and environmental patterns of phenotypic variation between the groups delimited by the molecular methods. Finally, we explored patterns of geographic and environmental isolation between the same groups. These can provide compelling evidence for reproductive isolation (Prates et al. 2024; Chambers et al. 2025). Furthermore, this step is necessary because molecular species delimitation methods tend to overestimate diversity (Sukumaran and Knowles 2017), and phenotypic variation may not be informative (cryptic species) or relevant for reproductive isolation (Singhal et al. 2018). Additional details on our workflow are provided in the following paragraphs. The code used for each analysis is available at the Dryad Digital Repository (https://doi.org/10.5061/dryad.tqjq2bwb0).

Molecular Sampling

We used the DArTseq (Diversity Arrays Technology [DArT], Canberra, Australia) platform to genotype 93 individuals from across the range of *V. tristis* (Fig. 1c). Based on the phylogeny of Brennan et al. (2021), we also sequenced samples of *V. glauerti* (2 individuals), *V. scalaris* (6 individuals), and *V. varius* (2 individuals) to root trees and test the monophyly of *V. tristis*. Tissue samples were sourced from the following Australian biological collections: Australian Biological Tissue Collection (ABTC), Australian Museum (AMS), Australian National Wildlife Collection (ANWC), Museum and Art Gallery of the Northern Territory (NTM), Museums Victoria (NMV), Queensland Museum (QM), and Western Australian Museum (WAM) (Supplementary Table S1; Supplementary Tables and Supplementary Figs. available at Zenodo: https://doi.org/10.5281/zenodo.15486213). DArTseq data have been used successfully for phylogeographic inference and species delimitation in numerous taxa (e.g., Georges et al. 2018; Chaplin et al. 2020; Esquerré et al. 2021; Binks and Byrne 2022; Mahony et al. 2022), including other *Varanus* (Pavón-Vázquez et al. 2022).

DArT's proprietary pipelines were used to generate data for 2 primary sets of individuals: one including *V. tristis* only and one that also included the outgroups. DArTseq achieves complexity reduction through digestion with restriction enzymes and size filtering followed by sequencing (Sansaloni et al. 2010; Kilian et al. 2012). The enzymes used for this project were EBPCR1 and NlaIII. After PCR, equimolar amounts of amplification products from each sample were pooled and applied to c-Bot (Illumina) bridge PCR for sequencing on the Illumina Hiseq2500. The sequencing (single end) was run for 77 cycles. Common prokaryotic contaminants were removed through an algorithm designed by DArT, which has been trained using sequences for numerous taxa. The alignments were annotated based on

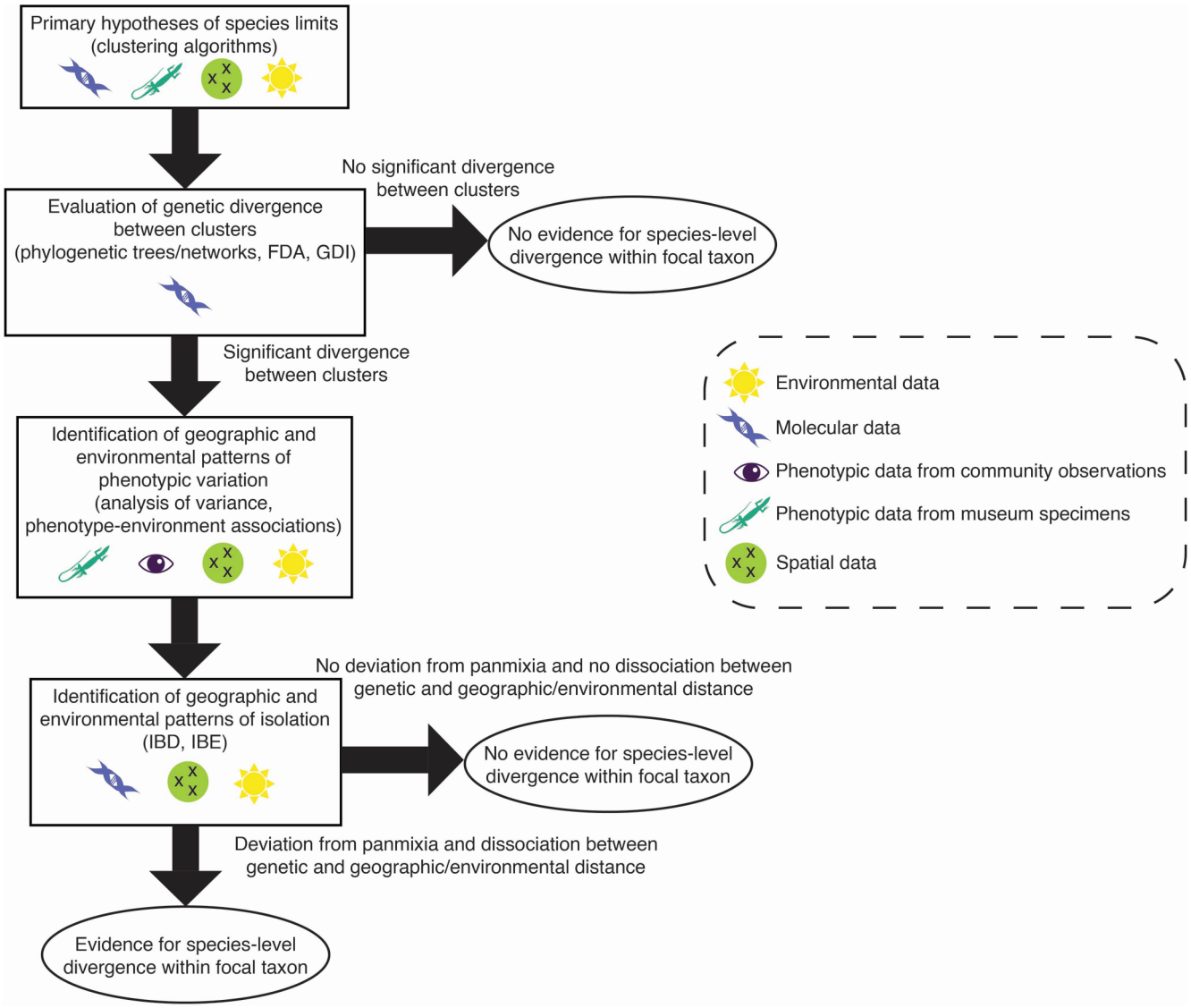

FIGURE 2. Workflow implemented here to delimit species in the *Varanus tristis* species complex. The general methods used in each step are indicated in parentheses. The sources of evidence used in each step are indicated by the icons.

the genome of *V. komodoensis* (BioProject PRJNA523222; Lind et al. 2019). The data sets delivered by DArT comprised 296,925 and 277,205 loci for the sets containing *V. tristis* only and the one that includes the outgroups, respectively. After trimming based on quality, DArTseq sequences are short (~69 bp) and contain at least one single-nucleotide polymorphism (SNP). We conducted additional filtering of loci and individuals on each data set to ensure data quality and meet the assumptions of the different analyses. In general, loci were filtered by reproducibility (>0.99) and call rate (>0.70), whereas individuals with high proportions of missing data (>0.70) were dropped (but see Supplementary Table S2 for details). Most processing was done in R 3.6.2 (R Core Team 2019) with the "dartR 1.8.3" package (Gruber et al. 2018). The raw reads have been deposited in the Sequence Read Archive (SRA; BioProject PRJNA1332121), and the data as delivered by DArT are available at the Dryad Digital Repository (https://doi.org/10.5061/dryad.tqjq2bwb0).

To detect potential mito-nuclear discordance as a result of introgression, we sequenced the mitochondrial NADH dehydrogenase subunit 4 protein (*ND4*) gene and the associated *tRNA-His*. We generated data for 44 individuals following the protocols described by Fitch et al. (2006). The purified PCR products were sequenced on an ABI Prism® 3700 DNA Analyzer at the Institute of Medical and Veterinary Science (IMVS), Adelaide, South Australia. We complemented these data with 32 sequences obtained from GenBank (Supplementary Tables S1 and S3). We aligned the sequences using the MUSCLE algorithm (Edgar 2004) and refined them by

hand in AliView 1.28 (Larsson 2014). The final alignment comprised 663 bp and included the following species (number of individuals in parentheses): *V. tristis* (45), *V. glauerti* (3), *V. glebopalma* (2), *V. hamersleyensis* (7), *V. mitchelli* (2), *V. pilbarensis* (7), *V. scalaris* (7), *V. semiremex* (2), and *V. spenceri* (1).

Phenotypic Sampling

We obtained 4 morphometric data sets: snout-vent length (SVL; used as proxy for body size); 17 linear measurements describing body shape; a two-dimensional geometric morphometric data set describing head shape in dorsal view, consisting of 13 landmarks and 20 sliding semi-landmarks; and a two-dimensional geometric morphometric data set describing head shape in lateral view, consisting of 10 landmarks (Pavón-Vázquez et al. 2022). All the data sets were recorded by the first author after examining specimens deposited across 7 herpetological collections: AMS, ANWC, NTM, QM, WAM, the South Australian Museum (SAMA), and the Natural History Museum, London (NHMUK) (Supplementary Tables S4–S6). Sexing was performed through dissection. All males larger than the smallest individual with enlarged testes, and all females larger than the smallest individual with vitellogenic follicles, were considered adults. Our sampling includes the types of *Odatria punctata* Gray 1838 (considered a synonym of *V. t. tristis*) and *Varanus punctatus* var. *orientalis* Fry 1913 (= *V. t. orientalis*). We processed the data mainly following Pavón-Vázquez et al. (2022). Briefly, missing measurements (i.e., from incomplete tails) were imputed using random forest training (Stekhoven and Bu¨hlmann 2012), and SVL was log-transformed. Body shape measurements were corrected for body size based on the allometric model of Thorpe (1975) using "GroupStruct 0.1.0" (Chan and Grismer 2021). We specified the "population2" option, which considers a single allometric slope for the whole data set. We did this to avoid introducing variation between populations a priori. We used generalized procrustes analysis (GPA) (Gower 1975) in "geomorph 4.0.0" (Baken et al. 2021; Adams et al. 2022) to standardize the geometric morphometric data sets. For each data set, we used the "procD.lm" function of "geomorph" to test for sexual dimorphism. For a data set exhibiting sexual dimorphism (body shape), we deleted females because our sampling is male-biased and repeated the allometric correction procedure afterward. Our final data sets included 62 (SVL, dorsal head shape), 45 (body shape), and 61 (lateral head shape) adults of *V. tristis*.

Additionally, we obtained head color data from the examined specimens and from photographic records issued by the wider public. We downloaded the photographic records using "galah 1.5.1" (Westgate et al. 2023), an R interface to the network of biodiversity living atlases. In our case, we downloaded the photographs and their associated metadata from the Atlas of Living Australia (Belbin et al. 2021). We did not include photographs with missing coordinates, where head coloration could not be clearly distinguished, and those of juveniles. The first author classified individuals into the following head color categories: "black," when any pattern (cephalic reticulation and dark postocular stripes) is mostly obscured by black pigment; "dim," when some patterning is visible, but the head is still noticeably darker than the rest of the body; "pale," when the head is light tan and the pattern is faded; "yellow," when the head is yellowish and the pattern is faded; and "freckled," when the head is light tan and the patterning is clearly visible on the head and neck. A map showing the distribution of the 5 color categories is shown in Supplementary Figure S1. However, in our analyses we collapsed the "black" and "dim" categories into a single "dark" category and the "pale" and "yellow" categories into a single "light" category. There were two reasons for this: one was to increase sample sizes, and the second was that it can be hard to tell apart the subcategories within the collapsed categories, particularly in preserved specimens. We included adults of both sexes in our analyses, after verifying that any given sex could show any of the patterns and that variation was basically geographical.

Identification of Clusters

We used a variety of methods to identify clusters of individuals. These clusters were used as operational units for downstream analyses aimed at testing their status as independent species. At this point, we did not assign clusters to a particular type of grouping of individuals or taxonomic category (population, metapopulation, subspecies, or species), instead relying on downstream analyses to reach taxonomic conclusions.

First, we used sNMF to identify clusters and estimate the ancestry coefficients of each individual. These analyses were performed on a filtered version of the *V. tristis* SNP data set containing 81 individuals and 35,162 SNPs (one SNP per DArT marker). Ancestry coefficients were calculated with sNMF (Frichot et al. 2014) in the "LEA 2.8.0" (Frichot and François 2015) R package. sNMF is an efficient and accurate method based on sparse nonnegative matrix factorization (Frichot et al. 2014). We selected the combination of the regularization (α) and tolerance (ε) parameters that minimizes cross-entropy between 18 possible combinations. For each combination, we performed 10 runs for each value of K (number of clusters) between 1 and 10. Subsequently, we performed 100 runs each for K 1–10 using the selected combination of α (1) and ε (0.00001). We extracted the ancestry coefficients from the run yielding the lowest cross-entropy. Additionally, we used principal component analysis (PCA) to visualize the genetic similarity between individuals in two-dimensional space. This was done with the "gl.pcoa" function of "dartR."

As a second approach, we used unsupervised machine learning to classify individuals in clusters using

approaches described by Derkarabetian et al. (2019). Specifically, we used unsupervised random forest in "randomForest 4.7.1.1" (Liaw and Wiener 2002). We scaled the data used as input for sNMF and implemented the random forest algorithm with 5000 trees. Multidimensional scaling (MDS) of the proximity matrix generated by random forest was performed using classic MDS (cMDS) and isotonic MDS (isoMDS) with the "MASS 7.3.58.1" R package (Venables and Ripley 2002). For each type of MDS, we performed two procedures to select the optimal number of clusters and classify individuals: 1) partitioning around medoids (PAM) clustering with the optimal number of clusters selected based on the gap statistic, using the "factoextra 1.0.7" package (Kassambara and Mundt 2020) (cMDS-GS and isoMDS-GS); and 2) clustering and selection of the number of clusters through hierarchical clustering in "mclust 6.1" (Scrucca et al. 2023) (cMDS-HC and isoMDS-HC), retaining two components as suggested by the broken stick method (Wang and Coombes 2025).

As another machine learning approach, we used a method based on self-organizing maps (SOM) (Kohonen 1998; Wehrens and Buydens 2007) that was recently used to identify potential species in a taxonomically challenging group (Pyron et al. 2023). SOM is an artificial neural network that reduces dimensionality based on similarity (Wehrens and Buydens 2007). Briefly, an input vector is projected into a two-dimensional output grid based on clustering in multidimensional space. Adjacency between cells in the output grid indicates similarity. After classifying observations into grid cells, *k*-means clustering can be used to identify the optimal number of clusters (i.e., species, in this context) (Wehrens and Buydens 2007; Pyron et al. 2023). Analyses were performed in the "kohonen 3.0.10" R package (Wehrens and Kruisselbrink 2018). We used the same data as for sNMF to calculate allele frequencies for each individual to be used as input. We specified an output grid with 9×9 cells so that each individual could potentially be classified into its own cell. We performed 50 replicates of the classifying algorithm, each consisting of 400 iterations and with a learning rate α (0.05, 0.01). Using *k*-means clustering, we selected the optimal number of clusters based on the maximum sequential decrease in the weighted sum of squares across all runs.

Finally, we used the SuperSOM approach to infer clusters of individuals based on the simultaneous analysis of multiple types of data. Unlike the SOM analyses presented above for the molecular data, SuperSOM can reduce dimensionality based on multiple input layers (Wehrens and Buydens 2007; Pyron 2023). Weighing of the layers is independent of scale or the amount of data in each layer. Our SuperSOM analysis was based on molecular, phenotypic, spatial, and environmental data. The latter two sets of variables are likely to reflect key biogeographic and ecological processes that contribute to population structure and lineage divergence, such as vicariance and local adaptation (Hua and Wiens 2013; Pavón-Vázquez et al. 2018; Pyron 2023). We implemented the approach of Pyron (2023) and used the scripts accompanying that publication, which rely primarily on the "kohonen" R package. Since the effects of missing data are poorly known (Pyron 2023), we conducted this analysis on 23 individuals for whom all types of data are available. This reduced sampling still sufficiently covers the geographic range of *V. tristis*. The *V. tristis* DArTseq data set was processed to ensure reproducibility and informativeness for this smaller sample (Supplementary Table S2). The spatial data included latitude, longitude, and elevation. The environmental data included mean solar radiation and climatic variables representing annual averages, extremes, and seasonality (bioclimatic variables 1, 4–6, and 12–15) at 30″ resolution (Fick and Hijmans 2017). The phenotypic matrix included log-scaled SVL, the allometrically corrected 17 linear measurements, the Procrustes-aligned coordinates of the head shape data sets (aligned anew for this set of individuals), and color (coded as 0 = dark, 0.5 = light, and 1 = freckled). All the nongenetic variables were scaled through min-max normalization. We specified 4×4 cells for the output grid and performed 100 replicate analyses, each consisting of 100 iterations with a learning rate α (0.5, 0.1). We follow Pyron (2023) and use the term "species coefficients" to denote the frequency of assignment of each individual to a particular cluster across the replicates.

Genetic Divergence between Clusters

We estimated the relationships between the individuals and clusters of *V. tristis* to estimate the history of divergence and relationships of the taxon in a phylogenetic context. Furthermore, phylogenetic hypotheses are required for some of our downstream analyses. First, we inferred the relationships between individuals based on the SNP data set that included outgroups, totaling 91 individuals and over 50,000 SNPs (Supplementary Tables S1 and S2). We implemented two approaches: concatenated maximum likelihood and a summary method based on the coalescent. We conducted the maximum likelihood analysis in IQ-TREE 1.6.8 (Nguyen et al. 2015). The Bayesian Information Criterion (BIC) was used to compare the fit of several substitution models that account for the ascertainment bias in SNP data sets (Kalyaanamoorthy et al. 2017). The BIC favored the TVM + F + ASC + R3 model. Support was calculated based on 1000 ultrafast bootstrap (UFB) replicates (Hoang et al. 2018) and site concordance factors (SCF) (Minh et al. 2020). The coalescent-based analysis was conducted in SVDquartets (Chifman and Kubatko 2014) as implemented in PAUP∗ 4.0 (Swofford 2003). We obtained bootstrap support (BS) based on 100 pseudoreplicates.

We estimated the relationships between the clusters identified by sNMF under a species tree approach using SVDquartets. We based this and subsequent analyses in this step on the sNMF clusters because that method recovered clusters that were highly concordant with geography and included a relatively large number of individuals each, in contrast to another method that recovered 10 clusters, 4 of which were represented by three or fewer individuals (see below). Furthermore, sNMF suggested more clusters than most other methods, providing a scheme that is adequate for estimating the relationships and patterns of gene flow between groups of individuals at a fine scale with a low risk of overlumping. How gene flow between non-sister lineages affects species tree estimation with SVDquartets remains poorly understood (Long and Kubatko 2018). Thus, to minimize the impact of gene flow in species tree inference, we only included individuals with ancestry coefficients $\geq$0.95 for a given cluster. We assigned two individuals of *V*. *scalaris* to their own taxon because they did not group with other *V*. *scalaris* in the individual-level analyses. We obtained BS based on 100 pseudo-replicates. We time-calibrated the resulting tree with MCMCTree in PAML 4.8 (Yang 2007), specifically using the approach that relies on approximate likelihood to efficiently calculate divergence times for large data sets (dos Reis and Yang 2011). For each cluster, we kept the individual with the fewest missing data. We specified the concatenated alignment (including invariant sites) as input (262,348 bp). We first estimated branch lengths using BASEML (Yang 2007). Time calibration relied on a secondary calibration based on the results of Brennan et al. (2021). We specified a uniform distribution with a soft bound on the maximum age. Specifically, we calibrated the split between *V*. *tristis* and *V*. *varius*, with minimum and maximum ages equaling 18 and 24 million years, respectively. The parameters of the distribution were calculated with "MCMCtreeR 1.1" (Puttick 2019). Inference was based on the HKY + G4 substitution model and a global clock model. The Dirichlet-gamma prior for the mean substitution rate was set to $\alpha = 1$ and $\beta = 18.7957$, based on the mean genetic distance between *V*. *varius* and the members of the *Odatria* subgenus of *Varanus* and the mean age of their most recent common ancestor (Brennan et al. 2021; Pavón-Vázquez et al. 2022). We performed 2 independent runs, each with 5000 burn-in iterations and 2 million post–burn-in iterations sampled every 100 iterations. We combined the runs after verifying convergence and that the effective sample size (ESS) for all parameters was above 200 in Tracer 1.7.2 (Rambaut et al. 2018).

We estimated an explicit network to infer migration between the sNMF clusters. Admixed individuals (i.e., those with ancestry coefficients <0.95 for any given sNMF cluster) were included in these analyses. *Varanus glauerti* was specified as the outgroup. Analyses were performed using TreeMix 1.13 (Pickrell and Pritchard 2012), a program that takes allele frequency data and detects migration edges (m) based on a Gaussian approximation to genetic drift. We specified a block size of 500 SNPs and ran 5 analyses for each value of m between 1 and 5. We used the "OptM 0.1.3" R package (Fitak 2021) to select the optimal number of m. This was based on a nonlinear least squares model, which had the best fit based on the Akaike Information Criterion (AIC). We verified that the 5 runs for the best value of m were consistent with each other.

To estimate the mitochondrial phylogeny, we implemented a Bayesian approach in BEAST 2.7.1 (Bouckaert et al. 2014). We used PartitionFinder (Lanfear et al. 2012) and ModelFinder (Kalyaanamoorthy et al. 2017) to find the optimal partitioning scheme (Chernomor et al. 2016) and corresponding substitution models. The best model included 3 partitions (best-fitting models in parentheses): the first codon position of *ND4* and *tRNA-His* (K3Pu + F + G4), the second codon position of *ND4* (TN + F + I), and the third codon position of *ND4* (TIM3 + F). We specified a coalescent constant population model and a strict clock. We time-calibrated the tree using a normal prior with a mean of 0.00805 substitutions/site/million years and a standard deviation of 0.001 (Bryson et al. 2012; Blair and Bryson 2017). We performed 2 independent runs, each consisting of 20 million generations with a sampling frequency of 1000. The runs were combined after assessing for convergence and ESS values above 200 in Tracer. We report the maximum clade credibility tree with 10% burn-in and common ancestor heights.

To identify diagnostic differences between clusters in the molecular data, we performed the fixed difference analysis (FDA) introduced by Georges et al. (2018). Gene flow involving only a small number of migrants per generation between randomly mating populations is sufficient to prevent allelic differences from becoming fixed (Wright 1931). Thus, fixed allelic differences between clusters are strong indicators of reduced gene flow (Kozak and Montanucci 2001; Georges et al. 2018). We tested for fixed differences between the clusters identified by sNMF using the "gl.fixed.diff" function of "dartR." The approach relies on simulation to account for the probability of false positives arising because of the incomplete sampling of clusters. We specified 1000 simulation iterations and considered differences as "fixed" if one allele is present in 100% of the individuals in one cluster and 0% of individuals in the other. We then repeated the analysis after collapsing the clusters that did not show significant fixed differences in the first round.

Finally, we calculated the genealogical divergence index (GDI) (Jackson et al. 2017; Leaché et al. 2019). The GDI of taxon A equals $1–e^{-2\tau AB/\theta A}$, where τAB is the divergence time between taxa A and B, and θA is the effective population size of A. Panmixia is indicated by GDI = 0, whereas GDI = 1 indicates complete isolation. Values below 0.2 are usually considered to indicate conspecificity, values between 0.2 and 0.7 are ambiguous,

and values above 0.7 are considered to be strong evidence for species-level divergence (Jackson et al. 2017; Leaché et al. 2019). We used BPP 4.1.4 (Flouri et al. 2018) to estimate θ and τ based on the sNMF clusters and used these estimates to get a posterior distribution of the GDI. We followed the approach of Leaché et al. (2019), where pairs of sister taxa are recursively collapsed based on their GDI. Given computational constraints, we performed the analysis on a random sample of 500 loci and 28 individuals selected to maximize the representation of genetic variation. The sequences were phased using fastPhase 1.4.8 (Scheet and Stephens 2006). We estimated parameters on the fixed cluster tree estimated by SVDquartets. The inverse-gamma distribution for the priors of θ and τ was based on the mean genetic distance within clusters and the mean distance between the earliest diverging cluster and the rest, respectively. For each round of testing, we conducted 2 analyses consisting of 100,000 burn-in iterations and 2 million post–burn-in iterations sampled every second iteration. The runs were combined after assessing convergence and verifying that the ESS for each parameter was above 200 in Tracer.

Phenotypic Variation

The FDA and GDI detected significant genetic divergence between 2 groups, which were also reciprocally monophyletic in our phylogenetic analyses and for which TreeMix did not detect migration. These groups were also consistently identified as distinct by the most conservative clustering analyses (isoMDS-GS, SOM, and SuperSOM). Thus, we treat these groups as putative species for the phenotypic analyses and those aimed at characterizing the geographic and environmental patterns of isolation (see below). We implemented analyses of variance to detect significant morphometric differences between the putative species. Those individuals that were sequenced were assigned to putative species as indicated by the molecular data. Other individuals were classified based on their geographic origin. For each linear measurement, namely SVL and the 17 body measurements, we used R to perform an ANOVA. For the multivariate data sets, including the body shape data set, we used the "procD.lm" function of "geomorph," relying on 10,000 iterations of residual randomization permutation (Collyer et al. 2015) for significance testing. To visualize the differences between the groups, we used boxplots for SVL and PCA for the multivariate data sets.

We examined patterns of geographic and environmental variation in head color, the key character used to propose a polytypic arrangement for *V. tristis*. Plotting of color variation in geographic space revealed that the "freckled" pattern is exclusively found in one of the putative species, while the other is polymorphic ("dark" or "light"). Our analyses were thus aimed at testing whether variation in the polymorphic lineage reflects gene flow and/or shared adaptive or plasticity mechanisms with the other lineage, suggesting their co-specificity. Alternatively, head color may instead vary independently in response to environmental factors within the polymorphic species, suggesting its evolutionary independence. To test this, we fitted Bayesian generalized nonlinear regression models in the "brms 2.19.0" R package (Bürkner 2017) to analyze color variation in the polymorphic species. We implemented a modified version of the approach described by Hantak et al. (2022). Color was indicated as a response variable under a Bernoulli distribution; that is, we modeled the probability of being light-colored. One of the predictors was the minimum geographic distance to freckled individuals. If light color is the result of ongoing gene flow or common adaptive/plasticity mechanisms with the freckled form, we anticipated that the probability of being light would increase with proximity to freckled individuals. We measured geographic distance as great-circle distance using the "codep 0.9.1" R package (Guenard et al. 2018). To test whether variation in the polymorphic species is being independently driven by the environment instead, we included the following predictors: latitude, elevation, annual mean solar radiation (averaged across months), and annual precipitation. Environmental rasters had 30″ resolution and were obtained from WorldClim2 (Fick and Hijmans 2017). Latitude was multiplied by –1, and all predictors were log-transformed and scaled. We also obtained annual mean temperature for each individual but did not include it in the models because it was tightly correlated ($R^2 \geq 0.40$) with other predictors. After deleting pseudo-replicates—individuals that were in the same raster cells as others—we retained 149 individuals. We fitted a total of 31 models specifying every possible combination of predictors. For each model, we ran 4 chains with 1000 burn-in iterations and 2000 post–burn-in iterations. We compared model fit using the leave-one-out cross-validation criterion (Vehtari et al. 2017). To evaluate how much variation is accounted for by the models, we calculated the Bayesian version of R^2 with the "bayes_R2" function. We plotted the conditional effects of the optimal model after verifying that adding interaction terms did not increase fit and that there was no significant spatial autocorrelation based on Moran's I using the "pgirmess 1.6.9" R package (Giraudoux 2018).

Geographic and Environmental Patterns of Isolation

We performed several analyses to test whether genetic distance between individuals increases gradually with geographic (IBD) and/or environmental distance (IBE). The detection of IBD and/or IBE would be indicative of a gradient of genetic differentiation within a single species. Alternatively, abrupt changes in genetic distance over geographic/environmental space

are indicative of physical or biological barriers to gene flow (Pavón-Vázquez et al. 2024; Prates et al. 2024).

We tested for IBD using a Mantel test as implemented by the "gl.ibd" function of "dartR." We used the $\hat{a}$ statistic (Rousset 2000) as our measurement of genetic distance, because it may be more appropriate than F_{ST}-based statistics when data points represent individuals instead of populations. This metric, derived from the probability of allelic identity within versus between individuals, does not depend on a priori population assignment and is robust to varying levels of structure and sampling density (Rousset 2000; Langin et al. 2015; Shirk et al. 2017). Geographic distances were based on the Mercator projection. To locate geographic regions where genetic similarity decays abruptly, we estimated the effective migration surface of *V. tristis* in EEMS 0.0.0.900 (Petkova et al. 2016). This is a model-based Bayesian approach that identifies deviation from IBD. We used average genetic dissimilarity as our measurement of genetic differentiation (Petkova et al. 2016) and divided mainland Australia into 500 demes. We conducted 3 independent runs consisting of 1.5 million burn-in iterations, 5 million post–burn-in iterations, and a thinning of 10,000. The runs were combined after assessing for convergence.

To quantify the relative contributions of geographic and environmental distance to genetic differentiation, we used generalized dissimilarity modeling (GDM). GDM uses I-spline functions to perform nonlinear regression between pairwise matrices (Ferrier et al. 2007). The approach has been extensively used to analyze community dissimilarity but has also gained popularity as a way to identify the drivers of genetic differentiation (e.g., Myers et al. 2019; Dool et al. 2022). We performed the analyses on the gdm v1.5.0.1 R package (Fitzpatrick et al. 2021). We specified scaled $\hat{a}$ as our measure of genetic dissimilarity and included geographic distance, group membership, and environmental variables as predictors. We classified individuals into the 2 groups treated as putative species based on their distribution and morphology (when available; Fig. 1), coding them as 0 and 1. The purpose of including group membership as a predictor is to test whether genetic structure in *V. tristis* as a whole is better explained by IBD/IBE or a sharp differentiation in genetic makeup consistent with species-level differentiation. Additionally, we extracted 19 bioclimatic variables (Fick and Hijmans 2017) for each point from rasters with 2.5′ resolution. In addition to the present environmental conditions, we also extracted the 19 variables from data sets of past climate obtained from PaleoClim (Brown et al. 2018). Genetic differentiation may show a stronger correlation with past climate than with present climate if the former drove divergence. The paleoclimatic data sets correspond to two periods expected to have had a profound impact on genetic structure: the Last Interglacial (LIG) (Otto-Bliesner et al. 2006) and Last Glacial Maximum (LGM) (Karger et al. 2021). We also obtained 16 variables for the mid-Pliocene warm period (3.205 Ma) (Hill 2015), as it roughly coincides temporally with the basal split within *V. tristis*. We conducted individual analyses for each climatic data set, specifying as predictors the first principal components of the climatic variables accounting for over 99% of variance. We partitioned the deviance explained by the GDM into the 3 major groups of variables (i.e., geographic distance, taxonomy, and environmental conditions). Additionally, we used the function "gdm.varImp" to perform significance testing on the model and variables based on 100 rounds of matrix permutation.

As an alternative approach to examine the relative effects of IBD and IBE, we performed multiple matrix regression with randomization (Wang 2013). We used the "MMRR" function of Wang (2013). We specified the same data used in GDM as input, applied min-max scaling to the geographic and environmental distances, and performed 1000 permutations for significance testing.

Results

Identification of Clusters

The sNMF analyses recovered six as the optimal value of *K* based on cross-entropy. The 6 clusters are as follows (Figs. 3a,b, Supplementary Table S7): a widespread cluster (WS), with a wide distribution in the Arid Zone; a southwest cluster (SW), from the Mediterranean areas in southwest Australia; a central cluster (CT), confined to the Central Ranges; a cluster found in the Top End (TE) in northern Australia; a southeastern cluster (SE) with a wide distribution within the Great Artesian Basin; and a northeastern cluster (NE), occurring east of the northern portions of the Great Dividing Range. WS shows signs of substantial admixture with each of the clusters where they approach each other, except for NE. Substantial admixture of WS with SE is restricted to a single individual from Lake Buchanan, Queensland. We did not find signs of admixture between NE and SE where they approach each other, even when our sampling includes a region of possible sympatry around Lake Buchanan. The PCA mirrored these results (Fig. 3c). Scores for the first principal component, accounting for 26.46% of variance, differentiate NE from other clusters. SE groups separately from the remaining clusters along the second principal component, accounting for 8.49% of variance. The Lake Buchanan individual is roughly halfway between the latter 2 clusters. The scores for the third principal component differentiate TE (Supplementary Fig. S2).

A variable number of clusters was recovered by the different clustering procedures based on the random forest output (number of clusters in parentheses): cMDS-GS (10), cMDS-GS (4), isoMDS-GS (2), and isoMDS-GS (6). Most of these clusters imperfectly matched the

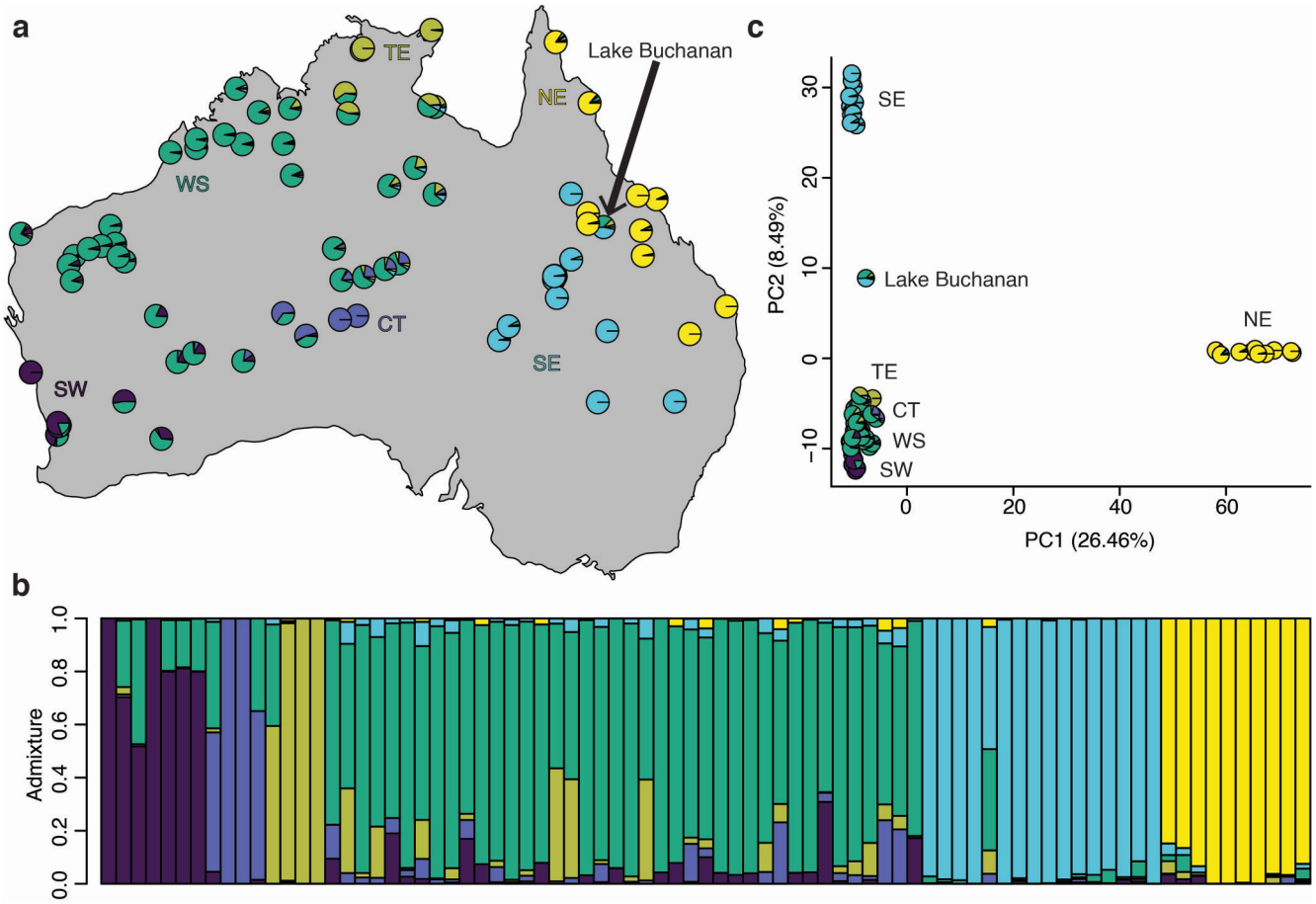

FIGURE 3. Genetic structure in *Varanus tristis*. a) Ancestry coefficients estimated with sNMF for $K = 6$; each pie chart represents an individual. b) Same ancestry coefficients as in (a), with bars corresponding to individuals. c) Principal component analysis of SNP data; pie charts indicate sNMF ancestry coefficients for individuals.

sNMF clusters (Fig. 4, Supplementary Table S7). However, all of the individuals assigned to NE by sNMF were consistently recovered as an independent cluster by all the methods based on the random forest results.

Forty-one of the cells in the 9 × 9 SOM output grid were occupied by 1–4 individuals each. Division into 2 clusters was supported by *k*-means clustering, because this value of *k* showed the largest decrease in the weighted sum of squares (both absolute and averaged) across 50 independent replicates (Supplementary Fig. S3). The resulting clusters corresponded to NE and the remaining sNMF clusters together (Fig. 4). The assignment probability of all individuals to their corresponding clusters was one, based on the 50 replicates.

In our SuperSOM analysis the molecular data had the largest scaled weight, followed by the phenotypic, climatic, and spatial data, in that order (Supplementary Fig. S3). Results support 2 clusters, corresponding to NE on one hand and the remaining clusters on the other (Figs. 4, Supplementary Fig. S3). Within the 4 × 4 output grid, 13 cells were occupied by 1–3 individuals each (Supplementary Fig. S3). Species coefficients for most individuals equaled one (Supplementary Fig. S3). For 2 individuals, a conflicting assignment was recovered by one run each. These individuals come from Gundabooka National Park, north-central New South Wales, and Lambert Creek, northeastern Queensland, respectively.

Genetic Divergence between Clusters

The individual-level trees obtained with SVDquartets (Fig. 5a, Supplementary Fig. S4) and IQ-TREE (Supplementary Fig. S4) were similar to each other. In both, *V. scalaris* was not monophyletic. Two samples of *V. scalaris* from the Wet Tropics of northeastern Queensland (hereafter *V. scalaris* WT) were recovered as sister to a clade containing *V. glauerti* and *V. tristis* with strong support. The reciprocal monophyly of the latter two taxa was also strongly supported. Samples assigned to NE

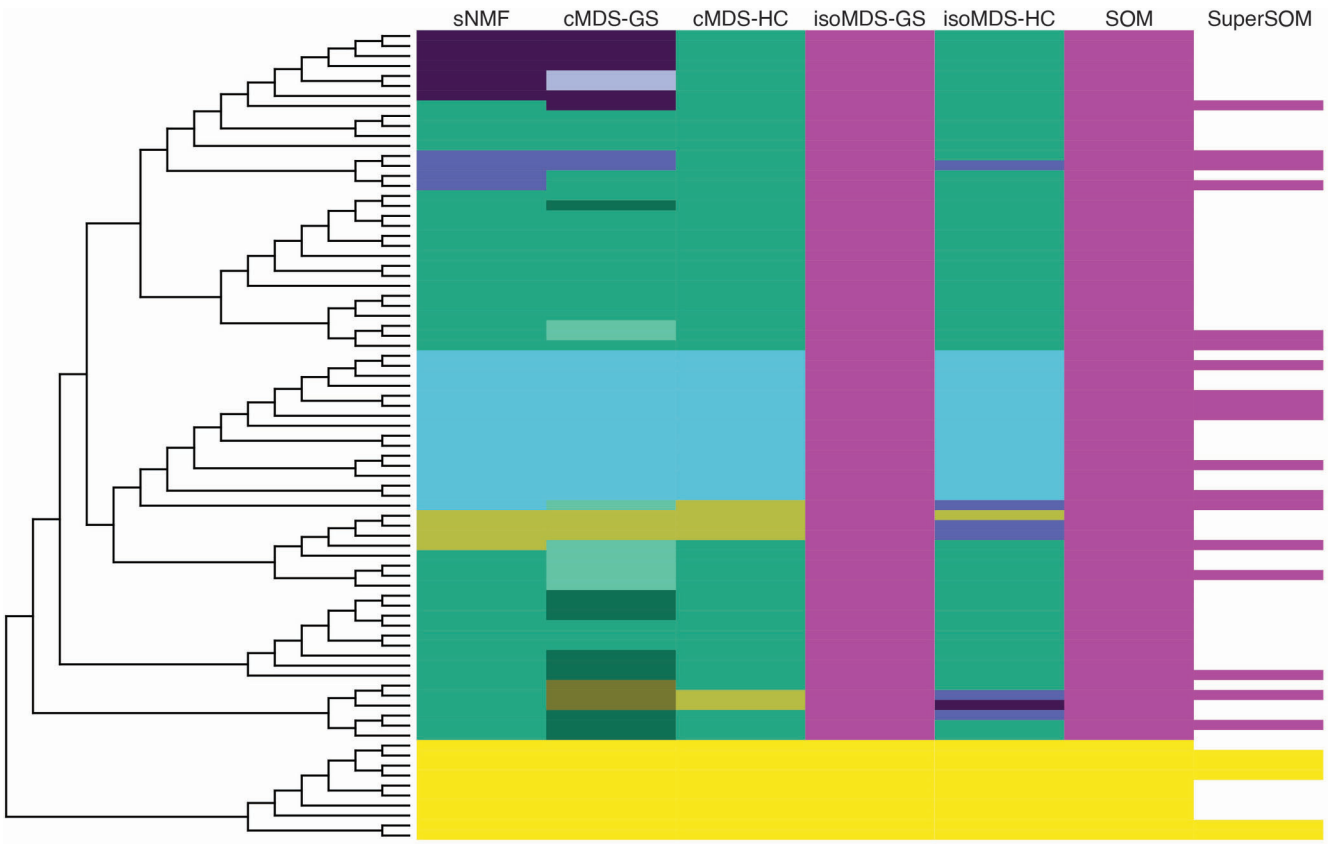

FIGURE 4. Clustering in *Varanus tristis* obtained by 7 methods. All methods based on genomic data, except for SuperSOM which also incorporated phenotypic, spatial, and environmental data. Each color represents a different cluster recovered by each of the methods. Relationships between individuals were estimated with SVDquartets (see main text; branch lengths are arbitrary).

compose a strongly supported clade that is sister to the rest of the sampled *V. tristis*. WS was not monophyletic. Instead, moderately to strongly supported clades corresponding to CT, SE, SW, and TE are nested within WS.

The cluster-level tree estimated with SVDquartets (Fig. 5b) also recovered *V. scalaris* WT as sister to *V. glauerti* + *V. tristis*, to the exclusion of other *V. scalaris*. Within *V. tristis*, NE was recovered as sister to the rest of the clusters. The clade comprising the latter clusters was strongly supported, but the relationships between them were not. SW and WS were recovered as sisters, whereas CT appeared as a sister to SE + TE. Dating suggests that the split between *V. glauerti* and *V. tristis* happened during the late Miocene (posterior mean [PM] = 5.52 Ma; 95% highest posterior density [HPD] = 4.63–6.48). The basal split within *V. tristis* likely happened during the Late Pliocene (PM = 2.99 Ma; 95% HPD = 2.46–3.55). Other divergences within the taxon were dated to the Pleistocene.

TreeMix (Fig. 5C) also recovered NE as a sister to a clade composed of the rest of the clusters. The topology recovered for the latter was (SE, (TE, (WS, (CT, SW)))). The nonlinear least squares model suggested that the optimal value of *m* was 2 (Supplementary Fig. S5). Migration was recovered from SW into WS and from CT into SE.

The mitochondrial tree (Supplementary Fig. S6) recovered *V. scalaris* WT as sister to topotypic *V. glauerti*, to the exclusion of other *V. scalaris*. Although the sister relationship between *V. scalaris* WT and *V. glauerti* was not strongly supported, a clade comprising *V. scalaris* WT, *V. glauerti*, and *V. tristis* was. A sample of *V. glauerti* from Arnhem Land in the TE was nested within *V. tristis*. That sample could not be included in the SNP analyses because the tissue sample was depleted and we could not locate any DNA extractions. Samples assignable to NE formed a strongly supported clade that was sister to the rest of *V. tristis* plus the *V. glauerti* sample from the TE. The latter sample appeared as sister to the rest of *V. tristis*, but its position was poorly supported. The remaining samples of *V. tristis* composed clades that roughly correspond geographically to the clusters recovered by sNMF. However, the sNMF clusters did not form reciprocally monophyletic groups. Divergence dates were generally older than those esti-

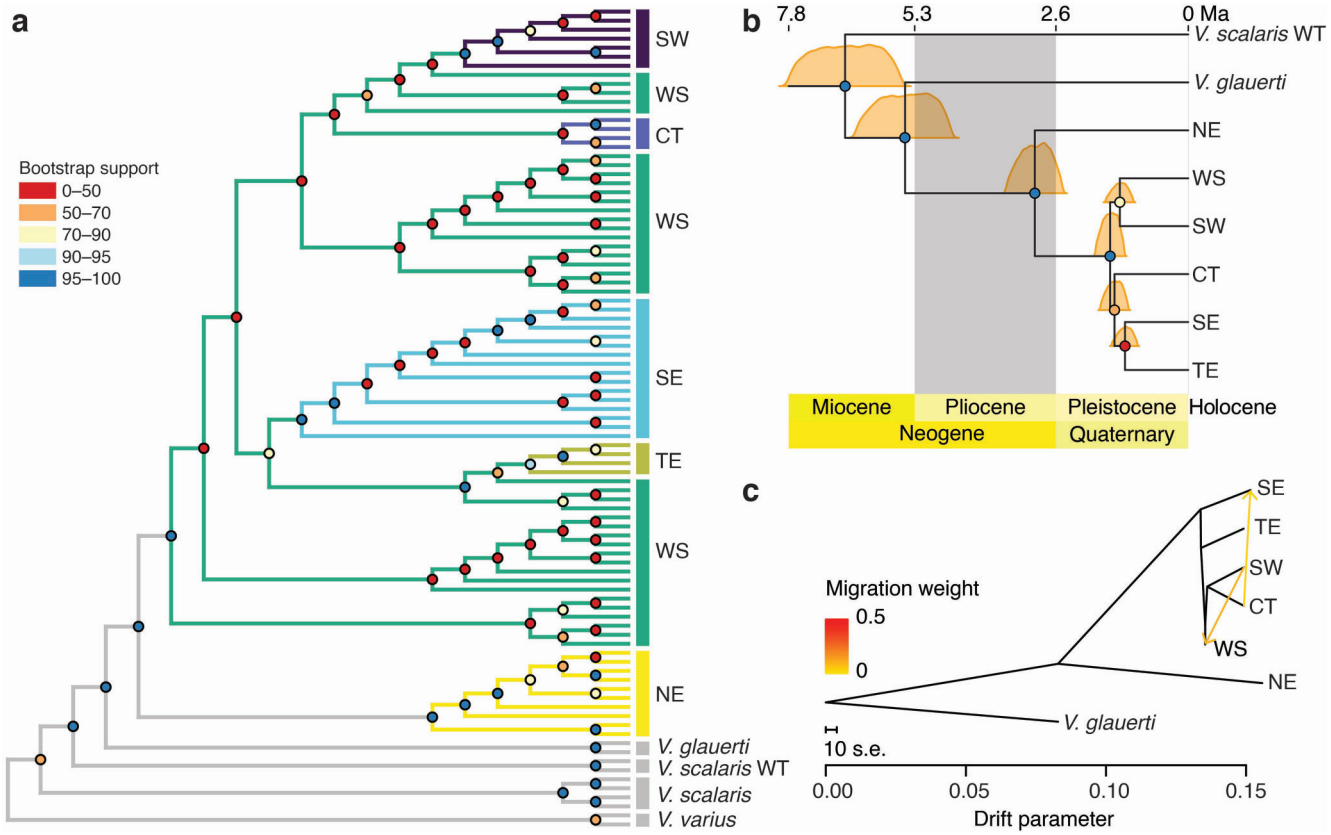

FIGURE 5. Phylogenomics of *Varanus tristis*. a) Individual-level phylogeny based on the SNP data and estimated with SVDquartets; circles at nodes indicate bootstrap support; branch lengths are arbitrary. b) Time-calibrated, cluster-level tree estimated with SVDquartets and calibrated with MCMCTree; posterior distributions of divergence times are shown for each node. c) Cluster network obtained with TreeMix under the optimal number of migration edges (two); branch lengths are proportional to estimated genetic drift between clusters; the smaller scale bar indicates 10 times the average standard error of the sample covariance matrix.

mated with the genomic data. The split between NE and its sister group was inferred to be 4.23 Ma old (95% HPD = 3.30–5.29). The most recent common ancestor of the remaining *V. tristis* was estimated to be 2.91 Ma old (95% HPD = 2.20–3.67).

The first round of FDA (Fig. 6a) detected significant fixed differences between NE and every other sNMF cluster. There were ≥9% fixed allelic differences between the former cluster and the others. After collapsing the remaining clusters into a single unit, we again found significant differences with NE ($P < 0.001$; fixed allelic differences = 8%).

Regarding the GDI analyses (Fig. 6b), NE had the highest GDI. The mean and most of the posterior distribution are above the 0.7 threshold, indicating strong evidence for speciation. Most of the other branches showed ambiguous values of GDI ($0.2 < \text{GDI} > 0.7$). Within this category, SE and the cluster comprising all the clusters except for NE had the highest GDI. Considering the results of the most conservative clustering algorithms, phylogenetic analyses, and species delimitation analyses, we treated NE and the rest of *V. tristis* as putative species in downstream analyses.

Phenotypic Variation

We found that while individuals of NE are generally smaller than other *V. tristis* (Fig. 7a), their mean SVLs were not significantly different ($F = 3.16$; $P = 0.0806$). Regarding our linear measurements describing body shape, we found significant differences in the length of the fourth finger ($F = 9.48$; $P = 0.0036$), hand width ($F = 4.10$; $P = 0.0490$), length of the fourth toe ($F = 6.98$; $P = 0.0114$), and foot width ($F = 14.07$; $P = 0.0005$). The multivariate analyses indicated significant differences in body shape ($F = 2.61$; $P = 0.0065$) (Fig. 7b), dorsal head shape ($F = 2.55$; $P = 0.0380$) (Fig. 7c), and lateral head shape ($F = 2.45$; $P = 0.0111$) (Fig. 7d). Other results are summarized in Supplementary Table S8.

Color variation in *V. tristis* (Fig. 8a) appears to be geographically structured. We found that the "freckled" pattern is found exclusively in northeastern Australia (Fig. 8b), corresponding to NE and the distribution of *V.*

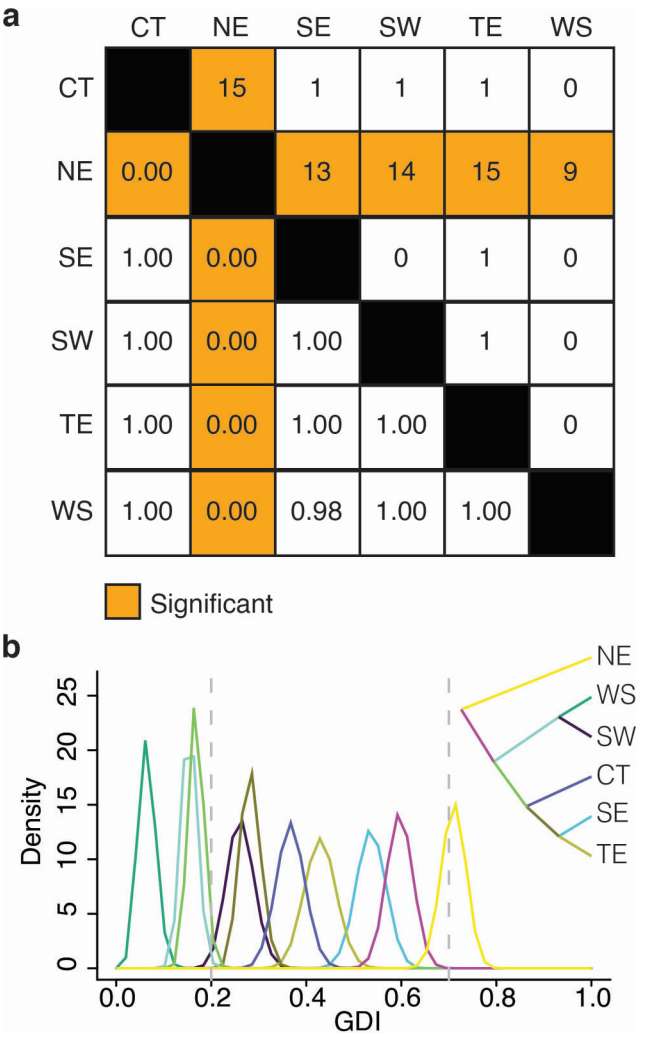

FIGURE 6. Genetic divergence within *Varanus tristis*. a) Fixed difference analysis; the upper triangle indicates the percentage of fixed allelic differences between clusters; the lower triangle indicates *p*-values based on simulations to account for false positives arising from sampling error; significant comparisons are highlighted. b) Posterior distribution of the GDI for each branch in the SVDquartets cluster-level tree; sister terminals were recursively collapsed based on their GDI; GDI < 0.2 suggests con-specificity, 0.2 < GDI > 0.7 indicates ambiguous results, and GDI > 0.7 suggests species-level divergence.

t. orientalis sensu Storr (1980). Variation in the remaining *V. tristis* appears to follow a latitudinal gradient (Fig. 8b). Light-colored individuals are mostly found in the northern portion of the distribution. Our Bayesian models corroborated this. The best-fitting model according to the leave-one-out cross-validation criterion was that including latitude and solar radiation as predictors (Supplementary Table S9). The PM of R^2 for this model is 0.65. The model suggests that there is a higher probability of observing light-colored individuals at higher latitudes and where solar radiation is less intense (Fig. 8c). The best-fitting model based on a single variable was that including latitude (expected log pointwise predictive density [elpd] difference with best model = 0.7; PM R^2 = 0.63). The model based exclusively on the geographic distance between the putative species performed poorly (elpd difference = –45.6; PM R^2 = 0.04). In fact, it had the worst fit according to the leave-one-out cross-validation criterion.

Geographic and Environmental Patterns of Isolation

The Mantel test revealed a significant positive relationship between genetic and geographic distance (r = 0.29; P = 0.001). However, visual inspection revealed that for similar geographic distances, the genetic distances between the putative species are disproportionately high (Fig. 9a, Supplementary Fig. S7). Similarly, effective migration rates (Fig. 9b) are particularly low in the geographic area separating NE from other *V. tristis*. This region corresponds to the border between the Great Dividing Range and the Great Artesian Basin. Other areas with low effective migration are found in the borders between the clusters identified by sNMF.

The GDM (Fig. 9c, Supplementary Tables S10–S12) indicated that group membership is a strong predictor of genetic disparity. Across all the time slices, the assignment to subspecies explained the largest proportion of the deviance in genetic distances, both independently and jointly with other variables. When taken independently, geographic distance explains a larger proportion of the deviance in genetic distances than climate. However, their joint contributions are comparable. Climate during the LGM explains a substantial proportion of the deviance in genetic distances compared with other points in time. The full models were significant across all time slices based on matrix permutations.

"MMRR" invariably calculated regression coefficients (β) that were significant and greater for geographic distance (β_D) than for environmental distance (β_E). The only significant contribution of climatic predictors to genetic variation was found in the MP data set ($\beta_{D\text{-Present}}$ = 1.47, P = 0.001; $\beta_{E\text{-Present}}$ = 0.11, P = 0.09; $\beta_{D\text{-LGM}}$ = 1.48, P = 0.001; $\beta_{E\text{-LGM}}$ = 0.1, P = 0.25; $\beta_{D\text{-LIG}}$ = 1.47, P = 0.001; $\beta_{E\text{-LIG}}$ = 0.11, P = 0.09; $\beta_{D\text{-MP}}$ = 1.38, P = 0.001; $\beta_{E\text{-MP}}$ = 0.21, P = 0.012).

DISCUSSION

Species Delimitation Workflow

Our workflow explores alternative explanations and accounts for confounding factors when exploring the observed patterns of genetic structure (IBD, IBE, incomplete lineage sorting, and gene flow) and phenotypic variation (polymorphism). We think these should be important considerations in species delimitation studies to avoid the taxonomic mischaracterization of diversity

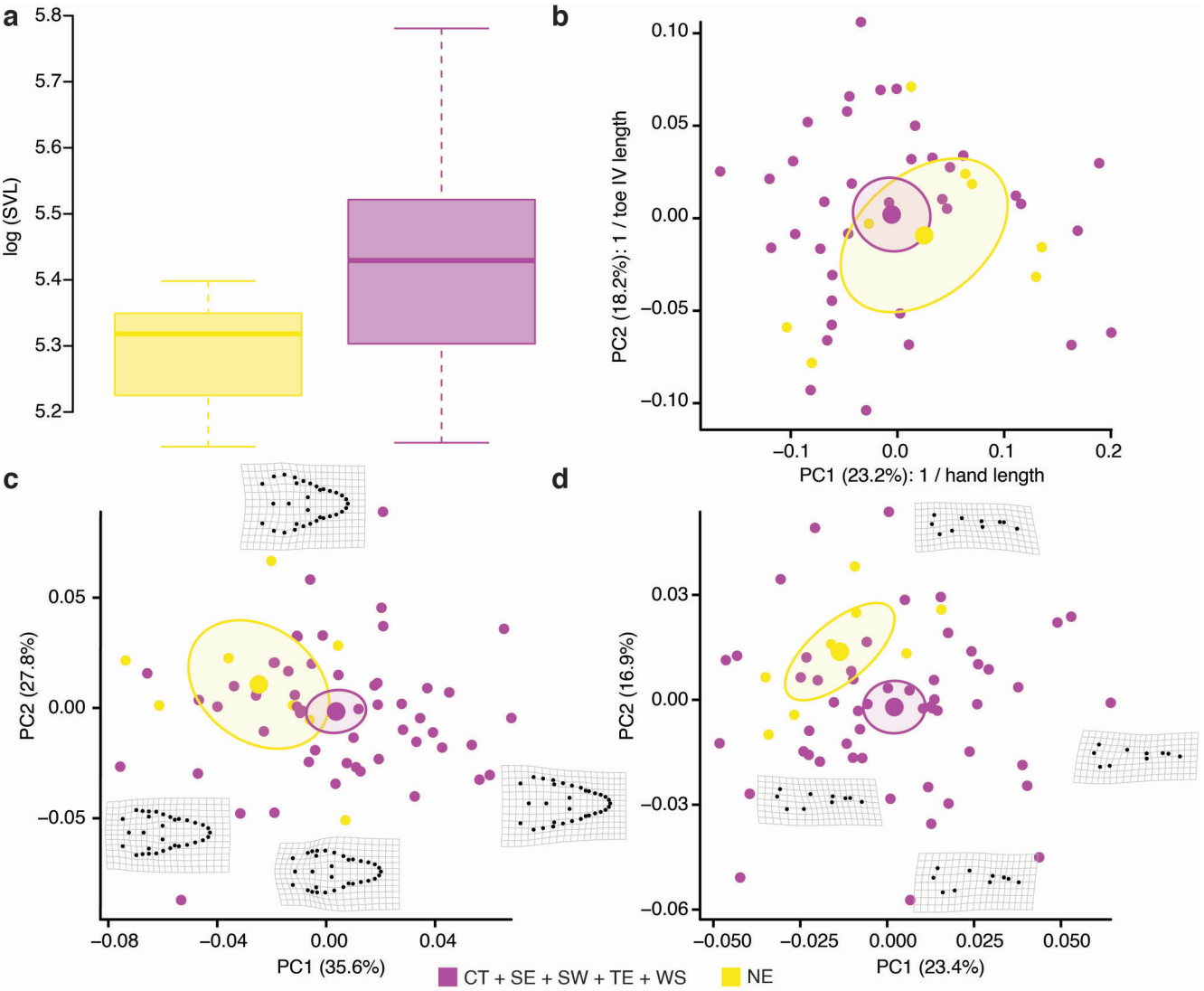

FIGURE 7. Morphometric variation in *Varanus tristis*. a) Boxplot of log-transformed snout-vent length (SVL); $n_{CT+SE+SW+TE+WS} = 37$, $n_{NE} = 8$. b) Plot of principal component analysis (PCA) for body shape; small points represent individuals, large points represent the mean for each putative species, circles indicate 95% confidence ellipses for the mean; the variables contributing the most to variation in each PC axis are shown; $n_{CT+SE+SW+TE+WS} = 37$, $n_{NE} = 8$. c) PCA plot for head shape in dorsal view; for the individuals at the extremes of each PC axis, the landmark configuration and deformation grid with respect to average shape are shown; $n_{CT+SE+SW+TE+WS} = 54$, $n_{NE} = 8$. d) PCA plot for head shape in lateral view; same as for (c); $n_{CT+SE+SW+TE+WS} = 53$, $n_{NE} = 8$.

(DeRaad et al. 2022; Pyron et al. 2023; Pavón-Vázquez et al. 2024; Chambers et al. 2025). Furthermore, explicitly stating the rationale behind each test and providing a clear workflow reinforces the concept of species as hypotheses (de Queiroz 2005), while also offering more straightforward guidelines for other researchers to test the results of species delimitation studies further. Delimiting species will invariably entail some degree of arbitrariness, as discrete criteria and thresholds have to be applied to a continuous and fractal pattern of divergence (Zachos 2016). However, clearly specifying the criteria used to separate taxonomic entities makes it easier for researchers and decision-makers to evaluate whether it is appropriate for them to incorporate taxonomic proposals from a practical perspective (e.g., whether to treat lineages as distinct units for macroevolutionary studies or conservation). Furthermore, studies that focus on evolutionary processes for species delimitation will produce valuable information about the biology of the organisms at hand and evolutionary processes in general, independently of their taxonomic conclusions.

Several aspects of our approach to species delimitation are worth discussing. First, we highlight that clustering algorithms that are not based on biological models should only be used to generate primary hypothe-

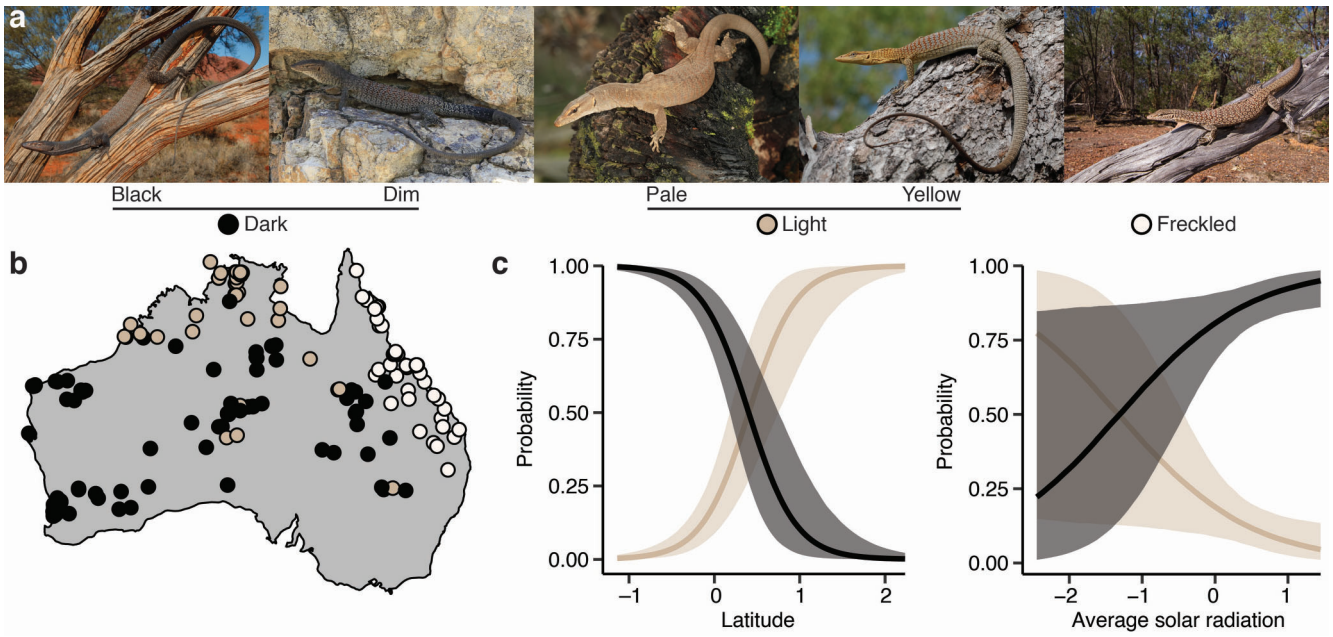

FIGURE 8. Color variation in *Varanus tristis*. a) Classification of variation into discrete categories; some categories were collapsed to increase sample sizes and because they were difficult to differentiate in preserved specimens; photographs by (left to right) Jules Farquhar, William Scott, Ryan Ellis, Jules Farquhar, and Stephen Zozaya. b) Geographic distribution of the 3 main color categories. c) Conditional effects under the best-fitting nonlinear model; the probability of being light or not was modeled, the probability of being dark was extrapolated from the former; shaded contours indicate 95% credible intervals; the predictors were log-transformed and scaled; geographic distance of dark and light individuals to freckled individuals was included in some models, but these were not favored.

ses of species limits ("species discovery") that need to be "validated" as species using downstream analyses (Carstens et al. 2013). Some methods, specifically isoMDS-GS, SOM, and SuperSOM, recovered clusters that likely match species in *V. tristis* (see below). However, until their behavior is more widely explored, they should not be treated as bona fide species delimitation methods. The methods used in our second step are imperfect for species delimitation. Monophyly can arise from IBD (Irwin 2002), and, on the other hand, species can be paraphyletic as they are the results of tokogenetic processes (Crisp and Chandler 1996). Fixed allelic differences can arise between populations or may take time to arise after speciation has occurred (Hudson et al. 2002; Rannala and Yang 2020). Inference of gene flow with TreeMix does not utilize all the information provided by genomic data sets, such as linkage disequilibrium, and can lose accuracy under certain circumstances (Wu 2020). The GDI can be biased by sampling and population sizes (Leaché et al. 2019). Thus, in our study, we used these methods to group the clusters recovered previously into putative species that were subsequently evaluated. Regarding the next step in our framework, we advocate for the inclusion of the phenotype because it embodies the interaction between organisms and their environment, reflecting how selection maintains species as cohesive entities (Cadena and Zapata 2021). However, we argue that the results of phenotypic analyses should not be interpreted in isolation. Failure to detect differentiation does not necessarily rule out speciation, and differentiation does not necessarily indicate speciation if it does not contribute to reproductive isolation (Singhal et al. 2018). However, speciation has probably occurred if phenotypic divergence is accompanied by evidence for reduced or no gene flow. That is why, in our workflow, the results of phenotypic analyses do not lead on their own to taxonomic conclusions but are instead used as supporting evidence. Finally, deviation from a continuous pattern of IBD or IBE is a strong indicator of barriers to gene flow, whether physical or biological (Pavón-Vázquez et al. 2024; Prates et al. 2024; Chambers et al. 2025). That is why we have placed it as the final validation of the species hypotheses generated and refined by the other steps in our approach.

The toolkit available to taxonomists has increased dramatically in recent years, enabling more efficient and comprehensive assessments of species boundaries. A major challenge for species delimitation is therefore the development of approaches that allow the integration of multiple data sources in biologically meaningful ways. Several emerging approaches show particular promise for transforming the way in which we discover and delimit species. Below, we highlight the opportunities and caveats associated with 2 tools that we have implemented here, which are expected to play a large role in species delimitation in the coming years: community science and machine learning. Additionally,

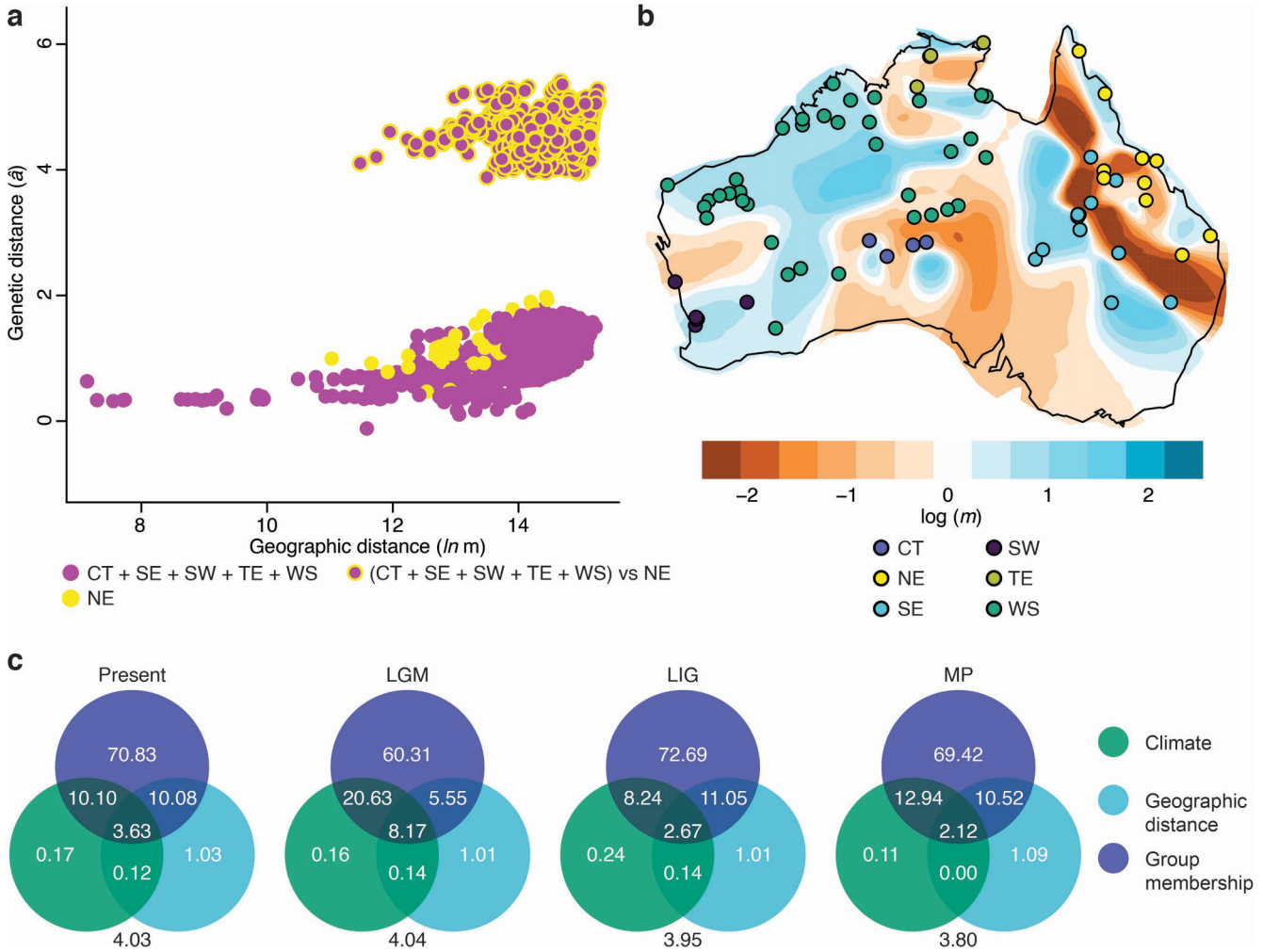

FIGURE 9. Patterns of isolation in *Varanus tristis*. a) Relationship between genetic and geographic distance; each point represents a pairwise comparison between individuals; comparisons are colored to allow comparison between 2 major clusters identified by isoMDS-GS, SOM, and SuperSOM (Fig. 4). b) Log-scaled effective migration rates (*m*); positive values indicate that *m* is larger than expected under isolation by distance, negative values indicate it is smaller; individuals are colored by sNMF cluster. c) Deviance in genetic distances explained by climate, geographic distance, and group membership obtained through generalized dissimilarity modeling; climatic variables were extracted from 4 points in time: the present, Last Glacial Maximum (LGM), Last Interglacial (LIG), and mid-Pliocene warm period (MP); circle centers show the deviance explained by each variable set alone, whereas intersections show the deviance explained by variable set combinations (adding all values within a circle gives the total deviance explained by each set; see Supplementary Table S10).

we discuss how multiple sources of information can be integrated to inform taxonomy as exemplified by *V. tristis*.

Integrating Community Science into Species Delimitation

Community observations can be used to address major gaps in our knowledge of biodiversity, namely about species' distributions (Wallacean shortfall) (Chowdhury et al. 2023a), abundance (Prestonian shortfall) (Robinson et al. 2018), traits and their functions (Raunkiæran shortfall) (Schiller et al. 2021), responses to abiotic conditions (Hutchinsonian shortfall) (Cheeseman et al. 2024), and interspecific interactions (Eltonian shortfall) (Maritz and Maritz 2020). As demonstrated here, community science also has the potential to become a major tool to address the Linnean shortfall—the incomplete knowledge of species diversity—especially when analyzed jointly with other sources of evidence and contrasted with evolutionary history. For instance, new species have been brought to the attention of taxonomists by community science projects (Winterton 2020; Zhang et al. 2022). Furthermore, records generated by the public can far outnumber those available in collections and better represent species ranges and therefore geographic variation (Chowdhury et al. 2023a).

Community observations can also harbor temporal, spatial, ecological, or even behavioral and acoustic in-

formation (Rowley et al. 2019). Thus, they have the potential to shed light on several aspects that are relevant for species delimitation, such as variation in mate recognition traits, temporal divergence in breeding activity, or phenotypes at contact zones. In this study, community observations boosted our sample sizes to test whether variation in head color—a variable and geographically structured trait in the focal taxon—reflects potential reproductive isolation. Specifically for *V. tristis*, we found that one color pattern ("freckled") is restricted to a genetic cluster, whereas a similar light-colored pattern in another lineage ("light") results from an independent cline of plasticity/adaptation, with the occurrence probability of that pattern not being correlated with proximity to the other cluster (Fig. 8; Supplementary Table S9). Thus, we found evidence for the evolutionary independence of each lineage (see below). In this way, community science accelerated taxonomic research in this taxon, as gathering the same amount of data through traditional means would necessitate additional fieldwork and/or museum visits, both of which require a significant investment of time and resources.

Despite the wealth of information provided by community observations on public platforms, certain limitations hinder their utility for taxonomic research. First, the precise location of threatened taxa is often obscured. This can have a significant impact on the estimation of species' ranges and their environmental preferences (Contreras-Díaz et al. 2023), both of which must be accurately characterized to contribute to precise species delimitation. This limitation could be ameliorated by putting procedures in place to facilitate access to obscured metadata by researchers. Moreover, the processing of a large number of records can pose practical challenges. This includes curating the taxonomic identification applied to each observation. However, the implementation of automated image processing workflows can accelerate this task (de Solan 2020; Hantak et al. 2022), representing one way among several in which artificial intelligence can aid taxonomy (see below). Additionally, the rate of taxonomic misidentification appears to be comparable between collection specimens and "research grade" iNaturalist observations (White et al. 2023). Finally, there are important taxonomic, spatial, temporal, and environmental biases in community observations (Rosa et al. 2022; Díaz-Calafat et al. 2024). In that context, scientific collections will remain essential for taxonomic research. Even if outnumbered by community records, collection records can provide a more comprehensive and accurate representation of biological diversity and its attributes (Eckert et al. 2024). Furthermore, the biases in collection records may differ from those in community observations, rendering them complementary. Thus, as in this study, we advocate for the combination of community and collection records in taxonomic research.

Another caveat associated with the use of photographs provided by the public is that they may fail to show relevant traits and are not captured under standardized conditions. The latter can misguide data collection, particularly for coloration traits. In our analyses, we addressed this limitation by classifying head color variation into categories that could consistently be differentiated. In turn, when color variation is coded as a quantitative trait, it appears that error introduced by the nonstandardization of community photographs is not directionally biased or predisposed towards certain colors (Luong et al. 2023). Additionally, depending on the research question and the way that color is scored, meaningful biological variation may be greater than error (Luong et al. 2023). Furthermore, as was the case in this study, taxonomically significant variation may be more easily distinguished from community photographs of live individuals than from museum specimens. This highlights the value of community photographs for ecological and evolutionary research using color (Medina et al. 2020; Farquhar et al. 2023; Jansen et al. 2025), including taxonomy (Fritz and Ihlow 2022).

Machine Learning and Species Delimitation

Artificial intelligence is rapidly evolving as a field, with the potential to greatly accelerate the discovery and description of biodiversity. Artificial intelligence has the potential to streamline the procurement of large phenotypic data sets in both museum collections and community science contexts. Machine learning can be used to quickly gather geometric morphometric data for many specimens with reduced error (Devine et al. 2020) and to extract phenotypic data from photographs obtained under different conditions, as is the case of community observations (de Solan 2020; Hantak et al. 2022). Machine learning can then be used to analyze these data solely or jointly with molecular data to assign them to known species with great accuracy (Wäldchen and Mäder 2018; Valan et al. 2019; Yang et al. 2022). Acoustic data can also be used to efficiently identify species in a deep learning framework (Kahl et al. 2021). These kinds of methods can then be extended to recognize variation that falls outside that expected for recognized taxa, that is, identify undescribed species (Yang et al. 2022).

Machine learning has also been incorporated explicitly into species delimitation frameworks. We implemented several approaches here (cMDS-GS, cMDS-HC, isoMDS-GS, isoMDS-HC, SOM, and SuperSOM). isoMDS-GS, SOM, and SuperSOM were the most conservative and appear to reflect species-level divergence as suggested by our downstream analyses. However, the behavior of these algorithms appears to be difficult to predict. In the study introducing the random forest-based methods implemented here, there was considerable congruence between the different algorithms, and they mostly recovered clusters that were consistent with

species (Derkarabetian et al. 2019). However, other studies (Martin et al. 2021) and our own (Fig. 4) found that the different algorithms showed notable variation in the number and individual composition of the recovered clusters. This likely reflects a susceptibility of the methods to variation in the data, filtering procedures, and the biological processes that shape genetic diversity, such as gene flow and incomplete lineage sorting (Martin et al. 2021).

On the other hand, SOM and SuperSOM appear to be more consistently conservative and robust to several evolutionary conditions (Pyron 2023; Burbrink et al. 2024). In our case, these methods were congruent with two widely used approaches for molecular species delimitation, FDA and GDI, as well as with patterns of phenotypic variation, IBD, and IBE. It is possible that SOM and SuperSOM simply recover higher-level groupings within the sampled individuals, in which case they may recover different types of biological groups depending on sampling. For instance, if the analyzed sample contained several deeply divergent species, they probably would recover the main clades. If the analyzed sample contained several individuals within a species, they would probably recover populations or metapopulations. Therefore, the accuracy of these methods in species delimitation could simply be the result of researchers including closely related species within a complex in their analyses. A thorough evaluation of the performance of SOM and SuperSOM with diverging data sets and under complex speciation scenarios, particularly those involving hybridization and gene flow, could offer clues on the robustness of these methods and on why they appear to recognize species-level divergence accurately.

A caveat associated with the use of unsupervised machine learning in species delimitation is that they do not estimate biological factors relevant for the recognition of species-level diversity, such as gene flow, phylogenetic relationships, or geographic/environmental patterns of phenotypic variation. Therefore, the clusters identified by these approaches cannot be confidently assigned to a particular type of ecological or evolutionary unit. Thus, we agree with Pyron (2023) and consider that unsupervised machine learning should be used as part of integrative frameworks where their results are validated through the characterization of biologically meaningful patterns and parameters.

A promising advance in the use of machine learning for species delimitation is the development of methods that rely on data simulated under a variety of evolutionary scenarios for training (e.g., Pei et al. 2018; Smith and Carstens 2020). These workflows mainly employ molecular data because the effects that evolutionary processes have on DNA have been relatively well studied. However, it is also possible to build models that can distinguish between intra- and interspecific phenotypic variation (Solís-Lemus et al. 2015). The utility of these models would be amplified if they were expanded to account for a greater variety of evolutionary scenarios, such as secondary contact and the reinforcement of reproductive isolation.

Species Limits and Variation in V. tristis

Our workflow revealed notable genetic structure and geographic variation in *V. tristis*, some likely representing species-level divergence. NE, in particular, was consistently recovered as a distinct cluster with minimal admixture with other clusters (Figs. 3 and 4). Downstream analyses allowed us to verify that this distinctiveness reflects its evolutionary independence. First, NE is sister to the rest of *V. tristis* in both the mitochondrial and nuclear phylogenies (Figs. 5, Supplementary Figs. S4 and S6), and the FDA and GDI reveal a high level of genetic divergence (Fig. 6). Furthermore, phenotypic differences were found in the morphometric data (Fig. 7) and more evidently in coloration (Fig. 8). Specimens assigned to NE can be distinguished by possessing a distinct dark postocular stripe and a reticulated dorsal pattern that extends anteriorly into the head. Geographic proximity with NE is not a good predictor of the presence of a light anterior coloration in the other clusters, in which this character seems to be environmentally driven (Fig. 8c). Finally, the genetic differentiation between NE and other *V. tristis* cannot be explained solely by IBD or IBE (Fig. 9), with group assignment being a better predictor of genetic divergence in the GDM. Particularly, genetic differentiation between NE and other clusters is dissociated from geographic distance (Fig. 9), constituting strong evidence for reproductive isolation (Prates et al. 2024).

The proposed intergradation between *V. t. tristis* and *V. t. orientalis* (Pianka 2004) is most likely the result of confusion regarding color variation in CT + SE + SW + TE + WS (see below). Moreover, the paraphyly of *V. t. orientalis* recovered by Fitch et al. (2006) is the result of labeling an individual from Noonbah Station, Queensland, as *V. t. orientalis*. In our study, both mitochondrial and nuclear data recovered that individual as a member of SE. Thus, multiple lines of evidence consistently indicate that NE forms a distinct evolutionary lineage. The type locality of *Varanus punctatus* var. *orientalis* Fry 1913 (Eidsvold, Upper Burnett River, Queensland) is within the range of NE, while that of *Monitor tristis* Schlegel 1839 (Swan River) is within the range of the remaining clusters. Therefore, we elevate the subspecies of *Varanus tristis* to the species level, using *Varanus orientalis* for NE and *Varanus tristis* for all the other clusters. We suggest the common names Freckled Monitor/Goanna and Black-tailed Monitor/Goanna, respectively.

The distribution of *V. orientalis* suggests that the Great Dividing Range played a major role in its divergence from *V. tristis*. However, the uplift of this mountain range started roughly 70 Ma (Taylor 1994), whereas we estimated *V. orientalis* to have diverged about 2.99 Ma during the Pliocene. Furthermore, portions of the

Great Dividing Range consist of low-elevation rolling hills (Johnson 2009), which are unlikely to represent a barrier to gene flow. However, the range creates a heterogeneous mosaic of climatic conditions and vegetation types (Taylor 1994). This heterogeneity is probably accentuated during periods of environmental change, fragmenting suitable habitats. A period of increased aridity and cooling is inferred to have occurred during the Pliocene (Bowler 1982). This had an impact on genetic structure in co-distributed taxa (Garrick et al. 2004) and provides a likely explanation for the divergence of *V. orientalis* that needs to be explored further.

Our results show that *V. tristis* as defined here (i.e., excluding *V. orientalis*) should be treated as a single, geographically structured species. Lineages are not reciprocally monophyletic, specifically because of the paraphyly of the widespread cluster (WS), and the FDA and GDI did not support the distinctness of the clusters that compose *V. tristis*. Admixture/gene flow is also apparent between WS and other clusters (Figs. 3a and 5c). In fact, WS appears to be connecting clusters that would mostly be isolated otherwise (see below).

IBD appears to be the main driver of divergence in *V. tristis* (Figs. 9, Supplementary Fig. S7). The GDM and "MMRR" also suggest that climate partially accounts for genetic differentiation in *V. tristis*, but that its relative relevance is temporally heterogeneous. In general, the Neogene and Quaternary in Australia are characterized by increased aridity, resulting in the expansion of dune fields and, counterintuitively, by the widespread presence of water bodies as a result of increased runoff (Pepper and Keogh 2021). All of these factors probably contributed to the fragmentation of the range of *V. tristis*. Approaches integrating genomics and paleoenvironmental data under a unified framework may shed additional light on the historic processes responsible for genetic divergence (Dolby et al. 2022).

Within *V. tristis*, SE appears to be the most highly differentiated cluster. The Carpentarian Gap, Simpson Desert, and Lake Eyre are all major barriers that probably restrict gene flow between SE and other clusters (Austin et al. 2013; Pepper and Keogh 2021; Pavón-Vázquez et al. 2022). However, occasional gene flow is apparently possible (Figs. 3 and 5c). We also found that mesic areas that may have functioned as refugia in the face of increasing aridity harbor endemic lineages (Pepper et al. 2011; Catullo et al. 2014; Dalmaris et al. 2015; Pepper and Keogh 2021). These are the TE region in the north, the Mediterranean regions in the southwest, and the Central Ranges (Figs. 1b and 3a). Although these clusters appear to be isolated from each other, they all show signs of admixture with a lineage that is widespread in the Arid Zone (Fig. 3a). A similar pattern was also found in another Australian monitor lizard (Pavón-Vázquez et al. 2022). This suggests that the expansion of arid-adapted lineages may have prevented or reversed speciation across several Australian taxa. Detailed demographic modeling is needed to test these hypotheses explicitly.

The variation in color exhibited by *V. tristis* is noteworthy and likely contributed to the taxonomic confusion in the complex. To further add to the confusion, the type localities of the former subspecies are located on opposite ends of the continent (some 3500 km away), and comparative material was scarce until the second half of the 20th century. In this study, we found that individuals assignable to SW are almost entirely Black (Schmida 2020), light-headed individuals are more prevalent in the Monsoonal Tropics but are also prevalent in the Central Ranges, and widespread clusters like WS and SE host both light- and dark-headed individuals (Fig. 8b). Our analyses indicate that color variation in *V. tristis* is probably not linked to gene flow with *V. orientalis* and is instead driven by environmental conditions. Particularly, it follows a well-established pattern where darker colorations are expected to be more common farther from the Equator (Gaston et al. 2008). This is termed the thermal melanism hypothesis, as it is thought that darker colors are more prevalent in colder climates because they allow individuals to gain heat faster (Clusella Trullas et al. 2007). This pattern is expected to be more prevalent in ectothermic organisms that rely largely on external sources of heat (Bogert 1949). Although we did not include temperature in our main analyses because it is tightly correlated with latitude, we confirmed that the probability of being dark-headed is negatively correlated with annual mean temperature (Supplementary Fig. S8). In fact, the latter variable accounts for more variation in color than any other tested predictor except for latitude (Supplementary Table S9). Intriguingly, we found that the probability of being dark-headed is higher in areas with higher annual mean solar radiation (Fig. 8c). However, this predictor fails to explain much of the color variation (Supplementary Table S9), and the 95% credible intervals of the conditional effects are wide (Fig. 8c).

Other Taxonomic Implications

The nuclear and mitochondrial data indicate that *V. scalaris* WT is more closely related to *V. glauerti*, *V. orientalis*, and *V. tristis* than to other *V. scalaris*. Additionally, the first author was able to examine 20 specimens assignable to *V. scalaris* WT. The taxon shows a cluster of enlarged scales on each side of the vent (spinose in adult males), a trait shared with *V. glauerti*, *V. orientalis*, and *V. tristis* and not found in *V. scalaris*. On the other hand, *V. scalaris* WT can be distinguished from *V. glauerti* by having a relatively shorter tail in adults (<65% of total length) and from *V. orientalis* and *V. tristis* by having the distal end of the tail banded. The name *Odatria kuranda* Wells and Wellington 1985 is available for this species. Wells and Wellington (1984, 1985) established numerous new names for Australian amphibians and reptiles, pre-

senting little or no evidence (Gans 1985; Grigg and Shine 1985; Shea and Sadlier 1999). Furthermore, several of the nomina that they established did not comply with the International Code of Zoological Nomenclature (Shea 1987). However, the International Commission on Zoological Nomenclature (ICZN) declined to suppress Wells and Wellington (1985) (ICZN 1991). Additionally, *Odatria kuranda* meets the minimum requirements for availability (Shea and Sadlier 1999) and has been used before in several publications (albeit between quotations) (Brown 2012; Schmida 2020). Kaiser et al. (2013) proposed that, beginning 1 January 2000, nomina need to be established following a combination of best scientific practices to be available. This proposal has been adopted by the Australian Society of Herpetologists (ASH 2022). However, the publication dates of Wells and Wellington (1984, 1985) mean that this proposition does not apply to them. Thus, we regrettably designate *V. scalaris* WT as *Varanus kuranda*, with the common name Spotted Rainforest Monitor/Goanna. However, it should be noted that the availability of the nomina created by Wells and Wellington (1984, 1985) needs to be critically evaluated on a case-by-case basis. We provide a distribution map for *V. kuranda* in Supplementary Figure S9.

Additional sampling is necessary to confidently evaluate the taxonomic status of *V. glauerti* from the TE. Morphologically, this population is clearly assignable to *V. glauerti* and distinct from *V. tristis*. Still, our mitochondrial tree suggests that this population is sister to *V. tristis*. Brennan et al. (2021) recovered similar results based on hundreds of nuclear loci. However, they only included the same single sample present in our mitochondrial tree. In the absence of additional data, it is difficult to evaluate alternative explanations for the phylogenetic placement of our single sample of *V. glauerti* from the TE, such as introgression or incomplete lineage sorting.

Conclusions

Our study demonstrates how community observations can be combined with genomic data and information from museum specimens to shed light on species limits. We analyzed these data through an integrative workflow to generate an updated taxonomy for a variable species complex. With human activities rapidly accelerating extinction (Barnosky et al. 2011), it is urgent to promptly but accurately characterize biodiversity. Community science and novel methods for the fast processing and analysis of data (such as machine learning) are likely to streamline species delimitation, allowing faster progress than that possible under traditional taxonomic practices. These strategies are likely to have a greater impact on taxonomic research in the Global South, where most megadiverse countries are located (Prathapan and Dharma Rajan 2020). Embracing these approaches may lead us into a more productive and equitable new era of biodiversity research based on global cooperation between communities and scientists.

Acknowledgments

We thank A.P. Amey, R.D. Bray, P.D. Campbell, P.J. Couper, G.M. Dally, A. Drew, M.R. Hutchinson, L. Joseph, C. Kovach, S. Mahony, J. Melville, J.J.L. Rowley, J.W. Streicher, S. South, J. Sumner, A. Velasco Castrillón, and J. Worthington Wilmer for the support provided during specimen examination in their respective institutions and for the loan of tissue samples; M. Arvizu Meza for helping with specimen examination; R.J. Ellis, J.E. Farquhar, K. Palmer, W. Scott, and S.M. Zozaya for sharing relevant photographs; D. Esquerré and J. Fenker for methodological suggestions; A. Kilian and M. Pepper for their help with sequencing.

Supplementary Material

The supplementary figures tables are available at Zenodo: https://doi.org/10.5281/zenodo.15486213.

Conflict of Interest

None declared.

Funding

This work was supported by an Australian Research Council Discovery grant [DP210100820 to J.S.K.] and the Australian Government Research Training Program [ANU-6147817 to C.J.P.V.].

Data Availability

Newly generated mitochondrial sequences and the nuclear raw reads were deposited in GenBank (accession numbers PX394145–PX394188) and the SRA (BioProject PRJNA1332121). All the original data and scripts necessary to reproduce the analyses reported in this study can be accessed through the Dryad link: https://doi.org/10.5061/dryad.tqjq2bwb0.

References

Adams D.C., Collyer M.L., Kaliontzopoulou A., Baken E.K. 2022. Geomorph: software for geometric morphometric analyses. R package version 4.0.4. Available from: https://cran.r-project.org/package=geomorph.

ASH. 2022. Position of the Australian Society of Herpetologist on the increasing proliferation of names for taxa without adequate diagnosis or description and published without the benefits of peer review. Australian Society of Herpetologists Inc., Position Statement Version 3. Available from: http://www.australiansocietyofherpetologists.org/ash-official-list-of-australian-species (accessed October 2, 2023).

Austin J.J., Joseph L., Pedler L.P., Black A.B. 2013. Uncovering cryptic evolutionary diversity in extant and extinct populations of the southern Australian arid zone Western and Thick-billed Grasswrens (Passeriformes: Maluridae: *Amytornis*). Conserv Genet 14(6):1173–1184.

Australian Society of Herpetologists Official List of Australian Species. 2025. Available from: http://www.australiansocietyofherpetologists.org/ash-official-list-of-australian-species (accessed August 28, 2025).

Baken E.K., Collyer M.L., Kaliontzopoulou A., Adams D.C. 2021. geomorph v4. 0 and gmShiny: enhanced analytics and a new graphical interface for a comprehensive morphometric experience. Methods Ecol. Evol. 12(12):2355–2363.

Barnosky A.D., Matzke N., Tomiya S., Wogan G.O., Swartz B., Quental T.B., Marshall C., McGuire J.L., Lindsey E.L., Maguire K.C., Mersey B., Ferrer E.A. 2011. Has the Earth's sixth mass extinction already arrived? Nature 471(7336):51–57.

Belbin L., Wallis E., Hobern D., Zerger A., 2021. The Atlas of Living Australia: history, current state and future directions. Biodivers. Data J. 9:e65023.

Bini L.M., Diniz-Filho J.A.F., Rangel T.F.L.V.B., Bastos R.P., Pinto M.P. 2006. Challenging Wallacean and Linnean shortfalls: knowledge gradients and conservation planning in a biodiversity hotspot. Divers. Distrib. 12(5):475–482.

Binks R.M., Byrne M. 2022. Species delimitation, hybridization and possible apomixis in a rapid radiation of Western Australian *Leptospermum* (Myrtaceae). Bot. J. Linn. Soc. 200(3):378–394.

Blair C., Bryson R.W. 2017. Cryptic diversity and discordance in single-locus species delimitation methods within horned lizards (Phrynosomatidae: *Phrynosoma*). Mol. Ecol. Resour. 17(6):1168–1182.

Bogert C.M. 1949. Thermoregulation in reptiles, a factor in evolution. Evolution 3(3):195–211.

Bouckaert R., Heled J., Kühnert D., Vaughan T., Wu C.-H., Xie D., Suchard M.A., Rambaut A., Drummond A.J. 2014. BEAST 2: a software platform for Bayesian evolutionary analysis. PLoS Comput. Biol. 10(4):e1003537.

Bowler J. 1982. Aridity in the Late Tertiary and Quaternary of Australia. In: Barker W.R., Greenslade P.J.M., editors. Evolution of the flora and fauna of arid Australia. Adelaide: Peacock Publications. p. 35–45.

Brennan I.G., Lemmon A.R., Lemmon E.M., Portik D.M., Weijola V., Welton L., Donnellan S.C., Keogh J.S. 2021. Phylogenomics of monitor lizards and the role of competition in dictating body size disparity. Syst. Biol. 70(1):120–132.

Brown D. 2012. A guide to Australian monitors in captivity. Burleigh: ABK Publications.

Brown J.L., Hill D.J., Dolan A.M., Carnaval A.C., Haywood A.M. 2018. PaleoClim, high spatial resolution paleoclimate surfaces for global land areas. Sc. Data 5:1–9.

Bryson R.W., García-Vázquez U.O., Riddle B.R. 2012. Diversification in the Mexican horned lizard *Phrynosoma orbiculare* across a dynamic landscape. Mol. Phylogenet. Evol. 62(1):87–96.

Burbrink F.T., Myers E.A., Pyron R.A. 2024. Understanding species limits through the formation of phylogeographic lineages. Ecol. Evol. 14(10):e70263.

Bürkner P.C. 2017. brms: an R package for Bayesian multilevel models using Stan. J. Stat. Softw. 80:1–28.

Cadena C.D., Zapata F. 2021. The genomic revolution and species delimitation in birds (and other organisms): why phenotypes should not be overlooked. The Auk 138(2):1–18.

Carstens B.C., Pelletier T.A., Reid N.M., Satler J.D. 2013. How to fail at species delimitation. Mol. Ecol. 22(17):4369–4383.

Catullo R.A., Lanfear R., Doughty P., Keogh J.S. 2014. The biogeographical boundaries of northern Australia: evidence from ecological niche models and a multi-locus phylogeny of *Uperoleia* toadlets (Anura: Myobatrachidae). J. Biogeogr. 41(4):659–672.

Chambers E.A., Lara-Tufiño J.D., Campillo-García G., Cisneros-Bernal A.Y., Dudek D.J., León-Règagnon V., Townsend J.H., Flores-Villela O., Hillis D.M. 2025. Distinguishing species boundaries from geographic variation. Proc. Natl. Acad. Sci. USA 122(19):e2423688122.

Chan K.O., Grismer L.L. 2021. A standardized and statistically defensible framework for quantitative morphological analyses in taxonomic studies. Zootaxa 5023(2):293–300.

Chan K.O., Hutter C.R., Wood P.L., Grismer L.L., Das I., Brown R.M. 2020. Gene flow creates a mirage of cryptic species in a Southeast Asian spotted stream frog complex. Mol. Ecol. 29(20):3970–3987.

Chaplin K., Sumner J., Hipsley C.A., Melville J. 2020. An integrative approach using phylogenomics and high-resolution X-ray computed tomography for species delimitation in cryptic taxa. Syst. Biol. 69:294–307.

Cheeseman A.E., Jachowski D.S., Kays R. 2024. From past habitats to present threats: tracing North American weasel distributions through a century of climate and land use change. Landsc Ecol. 39(5):1–20.

Chernomor O., Von Haeseler A., Minh B.Q. 2016. Terrace aware data structure for phylogenomic inference from supermatrices. Syst. Biol. 65(6):997–1008.

Chifman J., Kubatko L. 2014. Quartet inference from SNP data under the coalescent model. Bioinformatics 30(23):3317–3324.

Chowdhury S., Aich U., Rokonuzzaman M., Alam S., Das P., Siddika A., Ahmed S., Labi M.M., Marco M.D., Fuller R.A., Callaghan C.T. 2023a. Increasing biodiversity knowledge through social media: a case study from tropical Bangladesh. Bioscience 73(6):453–459.

Chowdhury S., Fuller R.A., Ahmed S., Alam S., Callaghan C.T., Das P., Correia R.A., Di Marco M., Di Minin E., Jarić I., Labi M.M., Ladle R.J., Rokonuzzaman M., Roll U., Sbragaglia V., Siddika A., Bonn A. 2023b. Using social media records to inform conservation planning. Conserv. Biol. 38(1):e14161.

Clusella Trullas S., van Wyk J.H., Spotila J.R. 2007. Thermal melanism in ectotherms. J. Therm. Biol 32(5):235–245.

Cogger H. 2014. Reptiles and amphibians of Australia. Collingwood: CSIRO Publishing.

Collyer M.L., Sekora D.J., Adams D.C. 2015. A method for analysis of phenotypic change for phenotypes described by high-dimensional data. Heredity 115(4):357–365.

Contreras-Díaz R.G., Nori J., Chiappa-Carrara X., Peterson A.T., Soberón J., Osorio-Olvera L. 2023. Well-intentioned initiatives hinder understanding biodiversity conservation: cloaked iNaturalist information for threatened species. Biol. Conserv. 282:110042.

Crisp M.D., Chandler G.T. 1996. Paraphyletic species. Telopea 6(4):813–844.

Dalmaris E., Ramalho C.E., Poot P., Veneklaas E.J., Byrne M. 2015. A climate change context for the decline of a foundation tree species in south-western Australia: insights from phylogeography and species distribution modelling. Ann. Bot. 116(6):941–952.

de Queiroz K. 2005. Different species problems and their resolution. Bioessays 27(12):1263–1269.

de Solan T., Renoult J.P., Geniez P., David P., Crochet P.A. 2020. Looking for mimicry in a snake assemblage using deep learning. Am. Nat. 196(1):74–86.

DeRaad D.A., McCormack J.E., Chen N., Peterson A.T., Moyle R.G. 2022. Combining species delimitation, species trees, and tests for gene flow clarifies complex speciation in scrub-jays. Syst. Biol. 71(6):1453–1470.

Derkarabetian S., Castillo S., Koo P.K., Ovchinnikov S., Hedin M. 2019. A demonstration of unsupervised machine learning in species delimitation. Mol. Phylogenet. Evol. 139:106562.

Devine J., Aponte J.D., Katz D.C., Liu W., Vercio L.D.L., Forkert N.D., Marcucio R., Percival C.J., Hallgrímsson B. 2020. A registration and deep learning approach to automated landmark detection for geometric morphometrics. Evol. Biol. 47(3):246–259.

Díaz-Calafat J., Jaume-Ramis S., Soacha K., Álvarez A., Piera J. 2024. Revealing biases in insect observations: a comparative analysis between academic and citizen science data. PLoS One 19(7):e0305757.

Dolby G.A., Bennett S.E.K., Dorsey R.J., Stokes M.F., Riddle B.R., Lira-Noriega A., Munguia-Vega A., Wilder B.T. 2022. Integrating Earth–life systems: a geogenomic approach. Trends Ecol. Evol. 37(4):371–384.
Dool S.E., Picker M.D., Eberhard M.J. 2022. Limited dispersal and local adaptation promote allopatric speciation in a biodiversity hotspot. Mol. Ecol. 31(1):279–295.
dos Reis M., Yang Z. 2011. Approximate likelihood calculation on a phylogeny for Bayesian estimation of divergence times. Mol. Biol. Evol. 28(7):2161–2172.
Drury J.P., Barnes M., Finneran A.E., Harris M., Grether G.F. 2019. Continent-scale phenotype mapping using citizen scientists' photographs. Ecography 42(8):1436–1445.
Eckert I., Bruneau A., Metsger D.A., Joly S., Dickinson T.A., Pollock L.J. 2024. Herbarium collections remain essential in the age of community science. Nat. Commun. 15(1):1–12.
Edgar R.C. 2004. MUSCLE: multiple sequence alignment with high accuracy and high throughput. Nucleic Acids Res 32(5): 1792–1797.
Edwards S.V., Birks S., Brumfield R.T., Hanner R. 2005. Future of avian genetic resources collections: archives of evolutionary and environmental history. The Auk 122(3):979–984.
Esquerré D., Donnellan S.C., Pavón-Vázquez C.J., Fenker J., Keogh J.S. 2021. Phylogeography, historical demography and systematics of the world's smallest pythons (Pythonidae, *Antaresia*). Mol. Phylogenet. Evol. 161:107181.
Farquhar J.E., Pili A., Russell W. 2023. Using crowdsourced photographic records to explore geographical variation in colour polymorphism. J. Biogeogr. 50(8):1409–1421.
Ferrier S., Manion G., Elith J., Richardson K. 2007. Using generalized dissimilarity modelling to analyse and predict patterns of beta diversity in regional biodiversity assessment. Divers. Distrib. 13(3):252–264.
Fick S.E., Hijmans R.J. 2017. WorldClim 2: new 1-km spatial resolution climate surfaces for global land areas. Int. J. Climatol. 37(12):4302–4315.
Fitak R.R. 2021. OptM: estimating the optimal number of migration edges on population trees using Treemix. Biol. Methods Protoc. 6(1):bpab017.
Fitch A.J., Goodman A.E., Donnellan S.C. 2006. A molecular phylogeny of the Australian monitor lizards (Squamata: Varanidae) inferred from mitochondrial DNA sequences. Aust. J. Zool. 54(4): 253–269.
Fitzpatrick M., Mokany K., Manion G., Nieto-Lugilde D., Ferrier S. 2021. gdm: generalized dissimilarity modeling. R package version 1.5.0-1. Avaialble from: https://CRAN.R-project.org/package=gdm.
Flouri T., Jiao X., Rannala B., Yang Z. 2018. Species tree inference with BPP using genomic sequences and the multispecies coalescent. Mol. Biol. Evol. 35(10):2585–2593.
Frichot E., François O. 2015. LEA: an R package for landscape and ecological association studies. Methods Ecol. Evol. 6(8): 925–929.
Frichot E., Mathieu F., Trouillon T., Bouchard G., François O. 2014. Fast and efficient estimation of individual ancestry coefficients. Genetics 196(4):973–983.
Fritz U., Grismer L.L., Asztalos M. 2023. Hybrid zones of *Natrix helvetica* and *N. natrix*: phenotype data from iNaturalist and genetics reveal concordant clines and the value of species-diagnostic morphological traits. Vertebr. Zool. 73:383–395.
Fritz U., Ihlow F. 2022. Citizen Science, taxonomy and grass snakes: iNaturalist helps to clarify variation of coloration and pattern in *Natrix natrix* subspecies. Vertebr. Zool. 72:533–549.
Fry D.B. 1913. On a *Varanus* and a frog from Burnett River, Queensland, and a revision of the variations in *Limnodynastes dorsalis* Gray. Rec. Aust. Mus. 10(2):17–34.
Gans C. 1985. Comment on two checklists. Herpetol. Rev. 16: 6–7.
Garrick R.C., Sands C.J., Rowell D.M., Tait N.N., Greenslade P., Sunnucks P. 2004. Phylogeography recapitulates topography: very fine-scale local endemism of a saproxylic "giant" springtail at Tallaganda in the Great Dividing Range of south–east Australia. Mol. Ecol. 13(11):3329–3344.
Gaston K.J., Chown S.L., Evans K.L. 2008. Ecogeographical rules: elements of a synthesis. J. Biogeogr. 35(3):483–500.
Georges A., Gruber B., Pauly G.B., White D., Adams M., Young M.J., Kilian A., Zhang X., Shaffer H.B., Unmack P.J. 2018. Genomewide SNP markers breathe new life into phylogeography and species delimitation for the problematic short-necked turtles (Chelidae: *E mydura*) of eastern Australia. Mol. Ecol. 27(24):5195–5213.
Giraudoux P. 2018. pgirmess: spatial analysis and data mining for field ecologists. R package version 1.6.9. Available from: https://cran.r-project.org/package=pgirmess.
Gower J.C. 1975. Generalized procrustes analysis. Psychometrika 40(1):33–51.
Gray J.E. 1838. Catalogue of the slender-tongued saurians, with descriptions of many new genera and species. J. Nat. Hist. 1:388–394.
Grigg G.C., Shine R. 1985. An open letter to all herpetologists. Herpetol. Rev. 16:96–97.
Gruber B., Unmack P.J., Berry O.F., Georges A. 2018. dartr: an r package to facilitate analysis of SNP data generated from reduced representation genome sequencing. Mol. Ecol. Resour. 18(3):691–699.
Guenard G., Legendre P., Pages B. 2018. codep: multiscale codependence analysis. R package version 0.9-1. Available from: https://cran.r-project.org/package=codep.
Hantak M.M., Guralnick R.P., Cameron A.C., Griffing A.H., Harrington S.M., Weinell J.L., Paluh D.J. 2022. Colour scales with climate in North American ratsnakes: a test of the thermal melanism hypothesis using community science images. Biol. Lett. 18(12):20220403.
Hill D.J. 2015. The non-analogue nature of Pliocene temperature gradients. Earth Planet. Sci. Lett. 425:232–241.
Hinojosa J.C., Koubínová D., Szenteczki M.A., Pitteloud C., Dincă V., Alvarez N., Vila R. 2019. A mirage of cryptic species: genomics uncover striking mitonuclear discordance in the butterfly *Thymelicus sylvestris*. Mol. Ecol. 28(17):3857–3868.
Hoang D.T., Chernomor O., Von Haeseler A., Minh B.Q., Vinh L.S. 2018. UFBoot2: improving the ultrafast bootstrap approximation. Mol. Biol. Evol. 35(2):518–522.
Hortal J., de Bello F., Diniz-Filho J.A.F., Lewinsohn T.M., Lobo J.M., Ladle R.J. 2015. Seven shortfalls that beset large-scale knowledge of biodiversity. Annu. Rev. Ecol. Evol. Syst. 46(1):523–549.
Hua X., Wiens J.J. 2013. How does climate influence speciation? Am. Nat. 182(1):1–12.
Hudson R.R., Coyne J.A., Huelsenbeck J. 2002. Mathematical consequences of the genealogical species concept. Evolution 56:1557–1565.
ICZN. 1991. Decision of the commission. Three works by Richard W. Wells and C. Ross Wellington: proposed suppression for nomenclatorial purposes. Bull. Zool. Nomenclat. 48:337–338.
Irwin D.E. 2002. Phylogeographic breaks without geographic barriers to gene flow. Evolution. 56(12):2383–2394
Jackson N.D., Carstens B.C., Morales A.E., O'Meara B.C. 2017. Species delimitation with gene flow. Syst. Biol. 66:799–812.
Jansen N., Pruijn N., Mayer M. 2025. Citizen observations shed new light on geographic variation in colour polymorphism of a widespread reptile. J. Biogeogr. 52(3):629–640.
Johnson D. 2009. The geology of Australia. Cambridge: Cambridge University Press.
Kahl S., Wood C.M., Eibl M., Klinck H. 2021. BirdNET: a deep learning solution for avian diversity monitoring. Ecol. Informat. 61:101236.
Kaiser H., Crother B.I., Kelly C.M.R., Luiselli L., O'Shea M., Ota H., Passos P., Schleip W.D., Wüster W., 2013. Best practices: in the 21st Century, taxonomic decisions in herpetology are acceptable only when supported by a body of evidence and published via peer-review. Herpetol. Rev. 44:8–23.
Kalyaanamoorthy S., Minh B.Q., Wong T.K., Von Haeseler A., Jermiin L.S. 2017. ModelFinder: fast model selection for accurate phylogenetic estimates. Nat. Methods 14(6):587–589.
Karger D.N., Nobis M.P., Normand S., Graham C.H., Zimmermann N.E. 2021. CHELSA-TraCE21k v1. 0. Downscaled transient temperature and precipitation data since the last glacial maximum. Clim. Past Discuss. 19(2):439–456.

Kassambara A., Mundt F. 2020. factoextra: extract and visualize the results of multivariate data analyses. R package version 1.0.7. Available from: https://CRAN.R-project.org/package=factoextra.
Kilian A., Wenzl P., Huttner E., Carling J., Xia L., Blois H., Caig V., Heller-Uszynska K., Jaccoud D., Hopper C., Aschenbrenner-Kilian M., Evers M., Peng K., Cayla C., Hok P., Uszynski G. 2012. Diversity arrays technology: a generic genome profiling technology on open platforms. In: Pompanon F., Bonin A., editors. Data production and analysis in population genomics. Methods in molecular biology, Vol. 888. Totowa: Humana Press. p. 67–89.
Kohonen T. 1998. The self-organizing map. Neurocomputing 21(1–3):1–6.
Kozak K.H., Montanucci R.R. 2001. Genetic variation across a contact zone between montane and lowland forms of the two-lined salamander (*Eurycea bislineata*) species complex: a test of species limits. Copeia 2001(1):25–34.
Lanfear R., Calcott B., Ho S.Y., Guindon S. 2012. PartitionFinder: combined selection of partitioning schemes and substitution models for phylogenetic analyses. Mol. Biol. Evol. 29(6):1695–1701.
Langin K.M., Sillett T.S., Funk W.C., Morrison S.A., Desrosiers M.A., Ghalambor C.K. 2015. Islands within an island: repeated adaptive divergence in a single population. Evolution 69(3): 653–665.
Larsson A. 2014. AliView: a fast and lightweight alignment viewer and editor for large datasets. Bioinformatics 30(22):3276–3278.
Leaché A.D., Zhu T., Rannala B., Yang Z. 2019. The spectre of too many species. Syst. Biol. 68:168–181.
Liaw A., Wiener M. 2002. Classification and Regression by randomForest. R News 2:18–22.
Lind A.L., Lai Y.Y.Y., Mostovoy Y., Holloway A.K., Iannucci A., Mak A.C.Y., Fondi M., Orlandini V., Eckalbar W.L., Milan M., Rovatsos M., Kichigin I.G., Makunin A.I., Johnson Pokorná M., Altmanová M., Trifonov V.A., Schijlen E., Kratochvíl L., Fani R., Velenský P., Rehák I., Patarnello T., Jessop T.S., Hicks J.W., Ryder O.A., Mendelson J.R., Ciofi C., Kwok P.-Y., Pollard K.S., Bruneau B.G. 2019. Genome of the Komodo dragon reveals adaptations in the cardiovascular and chemosensory systems of monitor lizards. Nat. Ecol. Evol. 3(8):1241–1252.
Long C., Kubatko L. 2018. The effect of gene flow on coalescent-based species-tree inference. Syst. Biol. 67(5):770–785.
Luong Y., Gasca-Herrera A., Misiewicz T.M., Carter B.E. 2023. A pipeline for the rapid collection of color data from photographs. Appl. Plant Sci. 11(5):e11546.
Mahony M.J., Hines H.B., Bertozzi T., Mahony S.V., Newell D.A., Clarke J.M., Donnellan S.C. 2022. A sixth species of northern *Philoria* (Anura: Myobatrachidae) from the uplands of the World Heritage forests of eastern Australia. Zootaxa 5104(2):209–241.
Mallet J. 2007. Subspecies, semispecies, superspecies. In: Levin S.A., editor. Encyclopedia of biodiversity. London: Academic Press. p. 523–526.
Manley D.L., Lichter Marck I.H., Peralta K., Castro Castro A., Wogan K.A., Whiting C.V., Powell A.M. 2025. *Oviculabiradiata*, a new genus of Compositae from Big Bend National Park in Trans-Pecos Texas. PhytoKeys 252:141–162.
Maritz R.A., Maritz B. 2020. Sharing for science: high-resolution trophic interactions revealed rapidly by social media. PeerJ 8:e9485.
Martin B.T., Chafin T.K., Douglas M.R., Placyk J.S., Birkhead R.D., Phillips C.A., Douglas M.E. 2021. The choices we make and the impacts they have: machine learning and species delimitation in North American box turtles (*Terrapene* spp.). Mol. Ecol. Resour. 21(8):2801–2817.
Mason N.A., Fletcher N.K., Gill B.A., Funk W.C., Zamudio K.R. 2020. Coalescent-based species delimitation is sensitive to geographic sampling and isolation by distance. Syst. Biodivers. 18(3): 269–280.
McKinley D.C., Miller-Rushing A.J., Ballard H.L., Bonney R., Brown H., Cook-Patton S.C., Evans D.M., French R.A., Parrish J.K., Phillips T.B., Ryan S.F., Shanley L.A., Shirk J.L., Stepenuck K.F., Weltzin J.F., Wiggins A., Boyle O.D., Briggs R.D., Chapin S.F., Hewitt D.A., Preuss P.W., Soukup M.A. 2017. Citizen science can improve conservation science, natural resource management, and environmental protection. Biol. Conserv. 208:15–28.
Medina I., Vega-Trejo R., Wallenius T., Symonds M.R.E., Stuart-Fox D. 2020. From cryptic to colorful: evolutionary decoupling of larval and adult color in butterflies. Evol. Lett. 4(1):34–43.
Mesaglio T., Callaghan C.T. 2021. An overview of the history, current contributions and future outlook of iNaturalist in Australia. Wildl. Res. 48(4):289–303.
Minh B.Q., Schmidt H.A., Chernomor O., Schrempf D., Woodhams M.D., Von Haeseler A., Lanfear R. 2020. IQ-TREE 2: new models and efficient methods for phylogenetic inference in the genomic era. Mol. Biol. Evol. 37(5):1530–1534.
Myers E.A., Xue A.T., Gehara M., Cox C.L., Davis Rabosky A.R., Lemos-Espinal J., Martínez-Gómez J.E., Burbrink F.T. 2019. Environmental heterogeneity and not vicariant biogeographic barriers generate community-wide population structure in desert-adapted snakes. Mol. Ecol. 28(20):4535–4548.
Nguyen L.T., Schmidt H.A., Von Haeseler A., Minh B.Q. 2015. IQ-TREE: a fast and effective stochastic algorithm for estimating maximum-likelihood phylogenies. Mol. Biol. Evol. 32(1): 268–274.
Online Zoological Collections of Australian Museums. 2025. Available from: https://ozcam.org.au (accessed August 28, 2025).
Otto-Bliesner B.L., Marshall S.J., Overpeck J.T., Miller G.H., Hu A., CAPE Last Interglacial Project members. 2006. Simulating Arctic climate warmth and icefield retreat in the last interglaciation. Science 311(5768):1751–1753.
Padula V., Bahia J., Stöger I., Camacho-García Y., Malaquias M.A.E., Cervera J.L., Schrödl M. 2016. A test of color-based taxonomy in nudibranchs: molecular phylogeny and species delimitation of the *Felimida clenchi* (Mollusca: Chromodorididae) species complex. Mol. Phylogenet. Evol. 103:215–229.
Pavón-Vázquez C.J., Esquerré D., Fitch A.J., Maryan B., Doughty P., Donnellan S.C., Keogh J.S. 2022. Between a rock and a dry place: phylogenomics, biogeography, and systematics of ridge-tailed monitors (Squamata: Varanidae: *Varanus acanthurus* complex). Mol. Phylogenet. Evol. 173:107516.
Pavón-Vázquez C.J., García-Vázquez U.O., Bryson R.W., Feria-Ortiz M., Manríquez-Morán N.L., de Oca A.N.-M. 2018. Integrative species delimitation in practice: revealing cryptic lineages within the short-nosed skink *Plestiodon brevirostris* (Squamata: Scincidae). Mol. Phylogenet. Evol. 129:242–257.
Pavón-Vázquez C.J., Rana Q., Farleigh K., Crispo E., Zeng M., Liliah J., Mulcahy D., Ascanio A., Jezkova T., Leaché A.D., Flouri T., Yang Z., Blair C. 2024. Gene flow and isolation in the arid Nearctic revealed by genomic analyses of desert spiny lizards. Syst. Biol. 73(2):323–342.
Pei J., Chu C., Li X., Lu B., Wu Y. 2018. CLADES: a classification-based machine learning method for species delimitation from population genetic data. Mol. Ecol. Resour. 18(5): 1144–1156.
Pepper M., Ho S.Y.W., Fujita M.K., Scott Keogh J. 2011. The genetic legacy of aridification: climate cycling fostered lizard diversification in Australian montane refugia and left low-lying deserts genetically depauperate. Mol. Phylogenet. Evol. 61(3): 750–759.
Pepper M., Keogh J.S. 2021. Life in the "dead heart" of Australia: the geohistory of the Australian deserts and its impact on genetic diversity of arid zone lizards. J. Biogeogr. 48(4):716–746.
Petkova D., Novembre J., Stephens M. 2016. Visualizing spatial population structure with estimated effective migration surfaces. Nat. Genet. 48(1):94–100.
Pianka E.R. 1971. Notes on the biology of *Varanus tristis*. West. Aust. Nat. 11:180–183.
Pianka E.R. 2004. *Varanus tristis*. In: Pianka E., King D., editors. Varanoid lizards of the world. Bloomington (IN): Indiana University Press. p. 477–487.
Pickrell J., Pritchard J. 2012. Inference of population splits and mixtures from genome-wide allele frequency data. PLoS Genet. 8(11):e1002967.

Pizarro A.K., DeRaad D.A., McCormack J.E. 2023. Temporal stability of the hybrid zone between *Calocitta* magpie-jays revealed through comparison of museum specimens and iNaturalist photos. Ecol. Evol. 13(3):e9863.
Pocock M.J., Tweddle J.C., Savage J., Robinson L.D., Roy H.E. 2017. The diversity and evolution of ecological and environmental citizen science. PLoS One 12(4):e0172579.
Prates I., Hutchinson M.N., Singhal S., Moritz C., Rabosky D.L. 2024. Notes from the taxonomic disaster zone: evolutionary drivers of intractable species boundaries in an Australian lizard clade (Scincidae: *C tenotus*). Mol. Ecol. 33(20):e17074.
Prathapan K.D., Rajan P.D. 2020. Advancing taxonomy in the Global South and completing the grand Linnaean enterprise. Magataxa 1(1):73–77.
Puttick M.N. 2019. MCMCtreeR: functions to prepare MCMCtree analyses and visualize posterior ages on trees. Bioinformatics 35(24):5321–5322.
Pyron R.A. 2023. Unsupervised machine learning for species delimitation, integrative taxonomy, and biodiversity conservation. Mol. Phylogenet. Evol. 189:107939.
Pyron R.A., O'Connell K.A., Duncan S.C., Burbrink F.T., Beamer D.A. 2023. Speciation hypotheses from phylogeographic delimitation yield an integrative taxonomy for Seal Salamanders (*Desmognathus monticola*). Syst. Biol. 72(1):179–197.
Pyron R.A., O'Connell K.A., Lemmon E.M., Lemmon A.R., Beamer D.A. 2022. Candidate-species delimitation in *Desmognathus* salamanders reveals gene flow across lineage boundaries, confounding phylogenetic estimation and clarifying hybrid zones. Ecol. Evol. 12(2):e8574.
R Core Team. 2019. R: A language and environment for statistical computing. Vienna: R Foundation for Statistical Computing, Available from: https://www.R-project.org/.
Rambaut A., Drummond A.J., Xie D., Baele G., Suchard M.A. 2018. Posterior summarization in Bayesian phylogenetics using Tracer 1.7. Syst. Biol. 67(5):901–904.
Rannala B., Yang Z. 2020. Species delimitation. In: Scornavacca C., Delsuc F., Galtier N., editors. Phylogenetics in the genomic era. No commercial publisher | Authors open access book. p. 5.5:1–5.5:18.
Robinson O.J., Ruiz-Gutierrez V., Fink D. 2018. Correcting for bias in distribution modelling for rare species using citizen science data. Divers. Distrib. 24(4):460–472.
Rosa R.M., Cavallari D.C., Salvador R.B. 2022. iNaturalist as a tool in the study of tropical molluscs. PLoS One 17(5):e0268048.
Rousset F. 2000. Genetic differentiation between individuals. J. Evol. Biol. 13(1):58–62.
Rowley J.J.L., Callaghan C.T., Cutajar T., Portway C., Potter K., Mahony S., Trembath D.F., Flemons P., Woods A. 2019. FrogID: citizen scientists provide validated biodiversity data on frogs of Australia. Herpetol. Conserv. Biol. 14:155–170.
Sansaloni C.P., Petroli C.D., Carling J., Hudson C.J., Steane D.A., Myburg A.A., Grattapaglia D., Vaillancourt R.E., Kilian A. 2010. A high-density Diversity Arrays Technology (DArT) microarray for genome-wide genotyping in *Eucalyptus*. Plant Methods 6(1):1–11.
Scheet P., Stephens M. 2006. A fast and flexible statistical model for large-scale population genotype data: applications to inferring missing genotypes and haplotypic phase. Am. J. Hum. Genet. 78(4):629–644.
Schiller C., Schmidtlein S., Boonman C., Moreno-Martínez A., Kattenborn T. 2021. Deep learning and citizen science enable automated plant trait predictions from photographs. Sci. Rep. 11(1):1–12.
Schlegel H. 1839. Abbildungen neuer oder unvollsta¨ndig bekannter Amphibien: nach der Natur oder dem Leben entworfen. Du¨sseldorf: Arnz & Comp .
Schmida G. 2020. A photographic guide to Australian monitors. Gold Coast: Blurb.
Schmitt C.J., Cook J.A., Zamudio K.R., Edwards S.V. 2019. Museum specimens of terrestrial vertebrates are sensitive indicators of environmental change in the Anthropocene. Phil. Trans. R. Soc. B 374(1763):20170387.
Scrucca L., Fraley C., Murphy T.B., Raftery A.E. 2023. Model-based clustering, classification, and density estimation using mclust in R. New York (NY): Chapman and Hall.
Sexton J.P., Hangartner S.B., Hoffmann A.A. 2014. Genetic isolation by environment or distance: which pattern of gene flow is most common? Evolution 68(1):1–15.
Shea G.M. 1987. Comment on the proposed suppression for nomenclatural purposes of three works by Richard W. Wells and C. Ross Wellington. Bull. Zool. Nomenclat. 44:257–261.
Shea G.M., Sadlier R.A. 1999. A catalogue of the non-fossil amphibian and reptile type specimens in the collection of the Australian Museum: types currently, previously and purportedly present. Tech. Rep. Aust. Mus. 15:1–91.
Shirk A.J., Landguth E.L., Cushman S.A. 2017. A comparison of individual-based genetic distance metrics for landscape genetics. Mol. Ecol. Resour. 17(6):1308–1317.
Singhal S., Hoskin C.J., Couper P., Potter S., Moritz C. 2018. A framework for resolving cryptic species: a case study from the lizards of the Australian Wet Tropics. Syst. Biol. 67(6):1061–1075.
Smith M.L., Carstens B.C. 2020. Process-based species delimitation leads to identification of more biologically relevant species. Evolution 74(2):216–229.
Solís-Lemus C., Knowles L.L., Ané C. 2015. Bayesian species delimitation combining multiple genes and traits in a unified framework. Evolution 69(2):492–507.
Stekhoven D.J., Bühlmann P. 2012. MissForest—non-parametric missing value imputation for mixed-type data. Bioinformatics 28(1):112–118.
Storr G.M. 1980. The monitor lizards (genus *Varanus* Merrem, 1820) of Western Australia. Rec. West. Aust. Mus. 8:237–293.
Sukumaran J., Knowles L.L. 2017. Multispecies coalescent delimits structure, not species. Proc. Natl. Acad. Sci. USA 114(7):1607–1612.
Swofford D.L. 2003. PAUP. Phylogenetic analysis using parsimony and other methods. Version 4. Sunderland: Sinauer Associates.
Taylor G. 1994. Landscapes of Australia: their nature and evolution. In: Hill R.S., editors. History of the Australian vegetation: cretaceous to recent. Cambridge: Cambridge University Press. p. 60–79.
Thorpe R.S. 1975. Quantitative handling of characters useful in snake systematics with particular reference to intraspecific variation in the Ringed Snake *Natrix natrix* (L.). Biol. J. Linn. Soc. 7(1):27–43.
Valan M., Makonyi K., Maki A., Vondráček D., Ronquist F. 2019. Automated taxonomic identification of insects with expert-level accuracy using effective feature transfer from convolutional networks. Syst. Biol. 68(6):876–895.
Vehtari A., Gelman A., Gabry J. 2017. Practical Bayesian model evaluation using leave-one-out cross-validation and WAIC. Stat Comput 27(5):1413–1432.
Venables W.N., Ripley B.D. 2002. Modern applied statistics with S. New York (NY): Springer.
Wäldchen J., Mäder P. 2018. Machine learning for image based species identification. Methods Ecol. Evol. 9(11):2216–2225.
Wang I.J. 2013. Examining the full effects of landscape heterogeneity on spatial genetic variation: a multiple matrix regression approach for quantifying geographic and ecological isolation. Evolution 67(12):3403–3411.
Wang M., Coombes K.R. 2025. Package "PCDimension": finding the number of significant principal components. R package version 1.1.14. Available from: https://CRAN.R-project.org/package=PCDimension.
Weber A.A.-T., Stöhr S., Chenuil A. 2019. Species delimitation in the presence of strong incomplete lineage sorting and hybridization: lessons from *Ophioderma* (Ophiuroidea: Echinodermata). Mol. Phylogenet. Evol. 131:138–148.
Wehrens R., Buydens L.M. 2007. Self-and super-organizing maps in R: the Kohonen package. J. Stat. Soft. 21(5):1–19.
Wehrens R., Kruisselbrink J. 2018. Flexible self-organizing maps in kohonen 3.0. J. Stat. Soft. 87(7):1–18.
Weiss M., Weigand H., Weigand A.M., Leese F. 2018. Genome-wide single-nucleotide polymorphism data reveal cryptic species within

cryptic freshwater snail species—the case of the *Ancylus fluviatilis* species complex. Ecol. Evol. 8(2):1063–1072.
Wells R.W., Wellington C.R. 1984. A synopsis of the class Reptilia in Australia. Aust. J. Herpetol. 1:73–129.
Wells R.W., Wellington C.R. 1985. A classification of the Amphibia and Reptilia of Australia. Aust. J. Herpetol. Supp. Ser. 1:1–61.
Westgate M., Kellie D., Stevenson M., Newman P. 2023. galah: biodiversity data from the Living Atlas Community. R package version 1.5.1. Available from: https://CRAN.R-project.org/package=galah.
White E., Soltis P.S., Soltis D.E., Guralnick R. 2023. Quantifying error in occurrence data: comparing the data quality of iNaturalist and digitized herbarium specimen data in flowering plant families of the southeastern United States. PLoS One 18(12): e0295298.
Winterton S.L. 2020. A new bee-mimicking stiletto fly (Therevidae) from China discovered on iNaturalist. Zootaxa 4816(3): 361–369.
Wright S. 1931. Evolution in Mendelian populations. Genetics 16(2):97–159.
Wu Y. 2020. Inference of population admixture network from local gene genealogies: a coalescent-based maximum likelihood approach. Bioinformatics 36(Suppl_1):i326–i334.
Yang B., Zhang Z., Yang C.Q., Wang Y., Orr M.C., Wang H., Zhang A.B. 2022. Identification of species by combining molecular and morphological data using convolutional neural networks. Syst. Biol. 71(3):690–705.
Yang Z. 2007. PAML 4: phylogenetic analysis by maximum likelihood. Mol. Biol. Evol. 24(8):1586–1591.
Zachos F.E. 2016. Species concepts in biology: Historical development, theoretical foundations and practical relevance. Berlin: Springer.
Zhang Y.M., Sasan K., O'kennon R.J., Kranz A.J. 2022. Discovery through iNaturalist: new species and new records of oak gall wasps (Hymenoptera: Cynipidae: Cynipini) from Texas, USA. Zootaxa 5168(1):63–74.

Syst. Biol. 75(3):468–492, 2026

https://doi.org/10.1093/sysbio/syaf064
Advance Access publication September 25, 2025